

Geometry Control of Recrystallized Silicon Wafers
for Solar Applications

by

Christopher W Ruggiero

B.S., Mechanical Engineering (2007)

Massachusetts Institute of Technology

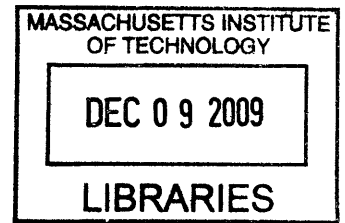
Submitted to the Department of Mechanical Engineering
in Partial Fulfillment of the Requirements for the Degree of
Master of Science in Mechanical Engineering

at the

Massachusetts Institute of Technology

June 2009

ARCHIVES



© 2009 Massachusetts Institute of Technology
All rights reserved.

A handwritten signature in black ink, appearing to read "C. W. Ruggiero".

Signature of Author.....
Department of Mechanical Engineering
May 7, 2009

Certified by.....
Emanuel M. Sachs
Fred Fort Flowers and Daniel Fort Flowers Professor of Mechanical Engineering
Thesis Supervisor

A handwritten signature in black ink, appearing to read "E. M. Sachs".

Accepted by.....
David Hardt
Professor of Mechanical Engineering
Graduate Officer

A handwritten signature in black ink, appearing to read "David Hardt".

Geometry Control of Recrystallized Silicon Wafers
for Solar Applications

by

Christopher W Ruggiero

Submitted to the Department of Mechanical Engineering
on May 7, 2009 in Partial Fulfillment of the
Requirements for the Degree of Master of Science in
Mechanical Engineering

ABSTRACT

The cost of manufacturing crystalline silicon wafers for use in solar cells can be reduced by eliminating the waste streams caused by sawing ingots into individual wafers. Professor Emanuel Sachs has developed a new method of manufacturing silicon wafers that consists of first, rapidly creating a low quality wafer, and then enhancing its electrical properties in a subsequent step. The result is a high-efficiency wafer produced without the need to saw an ingot into individual wafers. Our objective was to develop a method of encasing the wafer during the recrystallization step to retain the initial geometry of the wafer and eliminate the need for post-process sawing and grinding.

Initially, the silicon wafer was sandwiched between parallel Silicon Carbide backing plates during recrystallization, in an effort to preserve the wafer's initial thickness. This technique resulted in a recrystallized wafer with 212 μm of variation along the wafers length, and a normalized variation of $\sigma/\mu = 0.764$ (standard deviation divided by the mean thickness). To improve this variation, a new method was developed by creating a shell enclosure by sintering powder over the wafer and bottom backing plate. With the powder shell encasing technique, the variation was reduced to 28 μm across the wafer, and the normalized variation shrank to $\sigma/\mu = 0.125$.

A similar technique was also developed whereby the wafer was first coated in a ceramic slurry and subsequently embedded in a powder shell. The new technique resulted in slightly inferior thickness control than the powder shell technique with 64 μm of variation across the wafer's length and a normalized variation of $\sigma/\mu = 0.128$. However, the technique produced wafers with extraordinary surface finish, and proved to be quite robust in preserving fine detail, an added benefit that could be useful in production. Overall, if thickness variation could be reduced further with the ceramic coating technique, the added benefits that it creates would make it an excellent candidate for use in the recrystallization process.

Thesis Supervisor: Emanuel M. Sachs

Title: Fred Fort Flowers and Daniel Fort Flowers Professor of Mechanical Engineering

ACKNOWLEDGEMENTS

The author would first and foremost like to acknowledge Prof. Emanuel Sachs for his guidance in this process, developing me into a better engineer. His enthusiasm and unyielding vigor for making ideas work in practice has truly sparked a light in my intellectual desire.

The author would also like to thank Jim Serdy for his excellent assistance and ingenuity along the way. His unmatched ability in the lab not only aided my research, but has shown me techniques for solving any problem that comes forth.

Additionally, the author thanks Anjuli Appapillai and Eerik Hantsoo who've spent numerous hours improving the recrystallization process, and have passed invaluable insight on to me.

Table of Contents

ABSTRACT	3
ACKNOWLEDGEMENTS	5
Table of Contents.....	7
Chapter 1	9
Introduction	9
1.1 Energy Crisis.....	9
1.2 Cost of Solar Cells.....	11
1.3 Proposed Wafer Production Method	13
1.3.1 Initial Results	17
1.3.2 Proposed Method of Preserving Geometry	18
1.4 Powder Shell vs. Other Ideas.....	19
1.4 Overview and Important Considerations of Powder Shell	20
Chapter 2	24
Powder Shell Capsule Technique	24
2.1 General Sintering Theory and Problems	24
2.1.1 Sintering Basics.....	24
2.1.2 Shrinkage and Voids.....	26
2.2 Methods of Improving Sintering.....	27
2.2.1 Compaction: Reducing Voids and Increasing Packing Density	27
2.2.2 Bimodal Powders.....	31
2.3 Proposed Process for Recrystallization	35
2.3.1 Powder Selection.....	35
2.3.2 Powder Shell Creation Process	35
Chapter 3	38
Ceramic-Coating Technique.....	38
3.1 Current Technique and Sand Casting.....	38
3.2 Proposed Process for Recrystallization	39
Chapter 4	41

Measuring Thickness Uniformity	41
4.1 Beer’s Law: Relating Thickness and Transmission	42
4.2 Thickness Measuring Apparatus	44
4.3 Measurement Calibration.....	46
4.4 Contour Plot Generation.....	48
Chapter 5	50
Results and Evolution of Geometry Control	50
5.1 Control: Parallel Backing Plates	50
5.2 Powder Shell	52
5.3 Wafer Encased in Powder Shell.....	54
5.4 Powder Shell with Cast Release Layer.....	57
5.5 Ceramic Coating Technique	60
5.6 Additional Tests Using Ceramic Coating Technique.....	62
5.6.1 Detail Preservation	62
5.6.2 Recrystallization with Thinner Oxide Capsule	63
Chapter 6	66
Conclusions	66
References	68
Appendix A: Powder Selection	69
Testing Setup and Procedure	69
Single Constituent Powders.....	71
Bimodal Powders	77
Powder Comparison	82
Melting Tests	83

Chapter 1

Introduction

1.1 Energy Crisis

The world demand for energy is increasing and fossil fuels (which provide the majority of energy to the world) are running out. The biggest problem facing the world today is finding a renewable energy source to replace the world's rapidly depleting fossil fuel resources. The demand for energy is increasing at a staggering rate due to populations spiking across the globe and the increasing demand for higher living standards which require more energy in developing countries. According to *The Economist*, the global demand for oil will increase by 45% between 2006 and 2030.¹ This growth is broken down by regions of the world in Figure 1. This staggering growth in demand is concurrent with the supply of oil reaching a peak. This peak, originally suggested in Hubbert's Peak Theory, states that the supply of oil will only decrease moving forward (as a result of the depletion of reserves). As this mismatch in supply and demand grows, the price of oil will increase. This increase in the price of oil will have drastic impacts on the global economy specifically impacting food production and transportation. With this impending consequence, the need to find an alternative energy source becomes a paramount concern.

GROWING WORLD ENERGY DEMAND (millions of barrels per day)

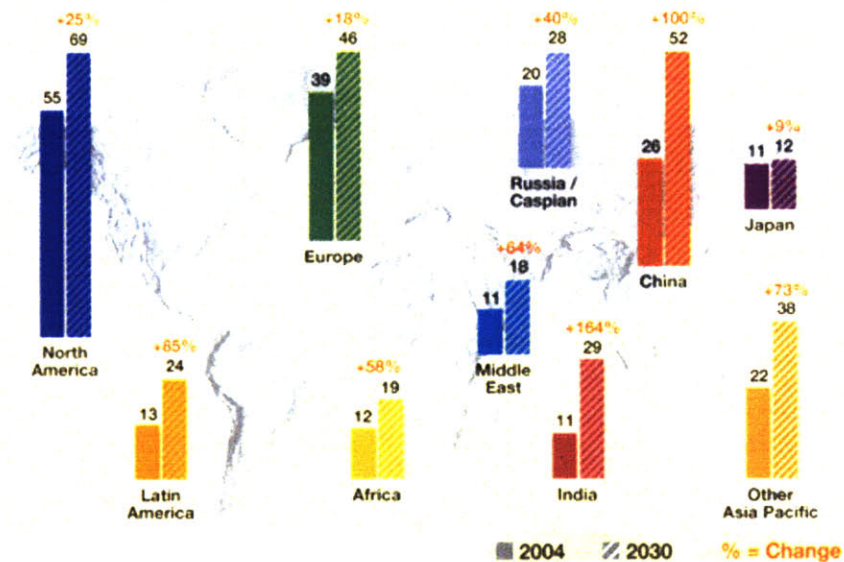


Figure 1: Map depicting the growth of energy demand from 2004 to 2030. The overall worldwide increase in demand is on the order of 45%.²

In addition to the economic need for an alternative energy source, environmental issues also exacerbate the need for a clean energy resource. “In the United States, more than 90% of greenhouse gas emissions come from the combustion of fossil fuels.”³ Coupled with this, the greenhouse gas concentration is “expected to rise due to ongoing burning of fossil fuels.”⁴ This increase in greenhouse gases has been observed to effect global temperatures, potentially impacting ecosystems across the globe. Additionally, the burning of fossil fuels generates nitric and sulfuric acid, that eventually fall to the ground as acid rain. This has detrimental effects on the environment and additionally is harmful to manmade structures. Finally, offshore oil drilling and mountainous coal mining destroys the surrounding environment.

The need for an alternative energy source is apparent, but the question becomes which renewable source is the best option to pursue. Figure 2 gives a comparison of the availability of various renewable resources. Solar flux is the largest renewable resource with 86,000 TW (TeraWatts) incident on the earth. Figure 2 also shows current global consumption, with the amount of incident solar energy at almost 6000 times the amount of total energy consumed. This enormous resource has far and away the most potential, but the question becomes how do we harness all of this energy?

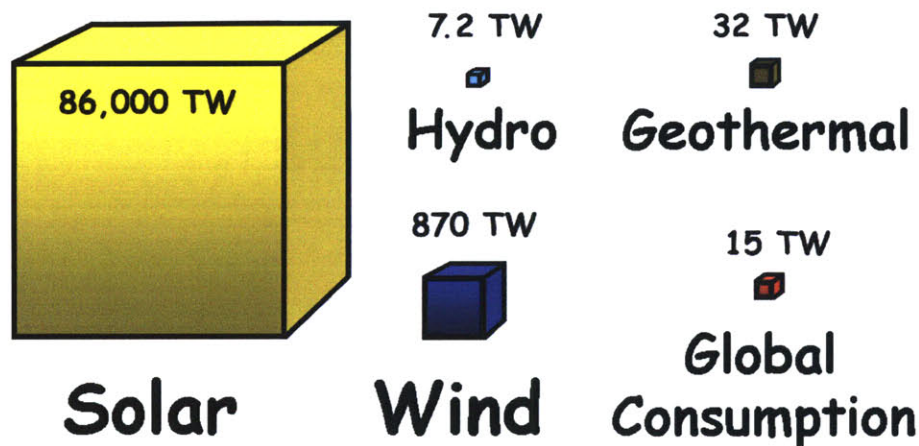


Figure 2: Schematic showing the availability of various renewable energy sources in Terawatts. The volume of each box depicts the available amount of each renewable source. Solar is far and away the most abundant resource.⁵

1.2 Cost of Solar Cells

Photovoltaic solar cells are ideal in that they produce electricity from sunlight with zero unwanted side effects. As shown in Figure 2, sunlight is an enormously available resource. Additionally, silicon, the main component of a traditional cell, is widely available as it is the second most abundant element in the earth's crust. There is no shortage of resources holding back solar cells from becoming prevalent, but rather, they cannot compete at a cost level to fossil fuels. To the end user, it costs about \$7.00/Watt of solar power, which does not compete with coal-generated electricity.

The majority of the cost of a complete solar cell comes from the cost of the silicon itself. Generally speaking, there are three types of silicon wafers used for crystalline silicon solar cells: mono-crystalline wafers, cast multi-crystalline wafers, and string ribbon wafers.

Mono-crystalline wafers produce high-quality solar cells with efficiencies in the 20% range. The main process used to manufacture monocrystalline silicon is the Czochralski process. The process entails dipping a seeded crystal fragment in a bath of molten silicon. The seed is then extracted and rotated, resulting in a cylindrical ingot composed of a single crystal. The cylinder is then sawn into discs or wafers onto which solar cells are created. The process is expensive and results in an undesirable waste stream from sawing the ingots into individual wafers.

Additionally, the circular disks produced must be cut further to produce a rectangular wafer to be packed in a solar module.

Cast multi-crystalline wafers generally produce less efficient solar cells but are much cheaper to produce. The process begins by pouring molten silicon into quartz crucible. The silicon is then directionally cooled to control grain growth and eventually a solid rectangular ingot is produced. This ingot is sliced into smaller ingots which are then sliced into wafers to be used as the backbone for PV devices. Abrasive wire sawing is the technique used to slice ingots into wafers resulting in an enormous waste stream of silicon. There has been an increasing desire for thinner wafers (< 200 um thick) to increase utilization, but this further increases waste from abrasive sawing.

A technique developed by Emanuel Sachs called String Ribbon, has focused on eliminating the need for sawing ingots into wafers. String ribbon is a process of drawing a multi-crystalline ribbon from a crucible of molten silicon. Since a ribbon of desired thickness is grown, the need to saw wafers is eliminated. Rather, the only post-processing needed to create wafers for use in solar cells is slicing the ribbon into rectangular wafers. The process eliminates much of the waste present in cast-multi wafers, but the result is a wafer with inferior electrical properties, and efficiencies less than that of cast-multi wafers.

The three current methods of producing silicon wafers for photovoltaic applications all have their tradeoffs. Mono-crystalline techniques provide high-efficiency cells, but at a high cost. Both multi-crystalline techniques are lower cost alternatives which result in lower cell efficiencies. Together, the three techniques can be plotted in a graph of wafer area per unit cost vs. efficiency. The graph is shown in Figure 3, and all three lie on the same line, with none shifting the curve outward to provide high efficiency cells at a low cost. String ribbon growth attempts to lower cost by eliminating the enormous waste from sawing cast-multi ingots into wafers. However, the electrical quality of such wafers is low enough to offset the cost savings of waste reduction. Therefore our goal is to produce a wafer of high electrical quality while simultaneously reducing waste streams (depicted in Figure 3 as the red box called “Cast Wafers”).

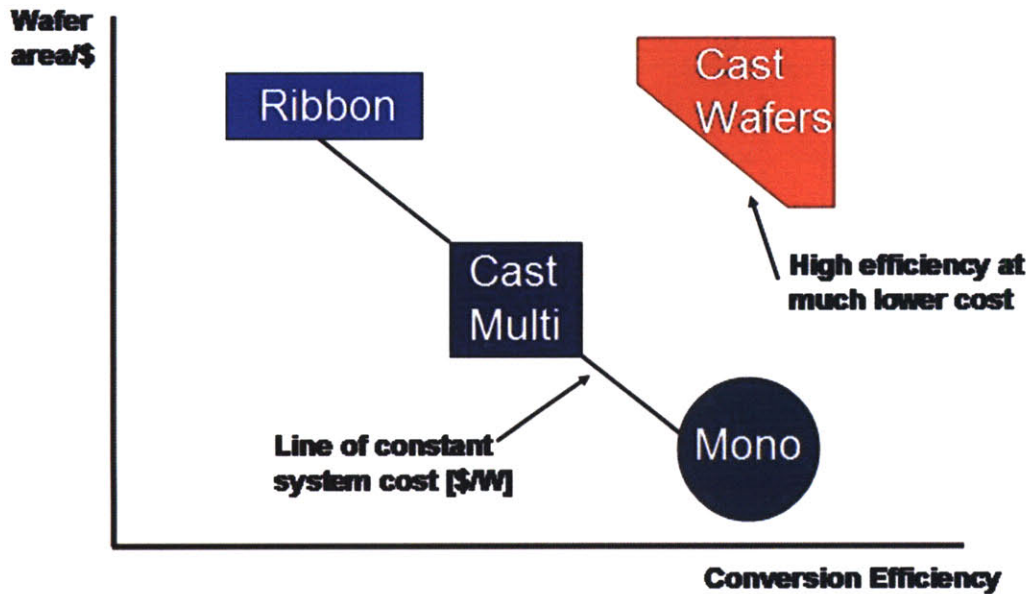


Figure 3: Plot of wafer area/\$ vs. conversion efficiency of solar cells created with silicon created with different manufacturing techniques. All three current techniques provide a tradeoff between efficiency and cost and lie along a line of constant system cost [\$/W]. The proposed technique aims to create high efficiency solar cells at a much lower cost, moving away from the line of constant system cost (diagram borrowed from proposal by Emanuel Sachs).

1.3 Proposed Wafer Production Method

Ely Sachs has developed a new wafer manufacturing process that aims to produce cast-multi high-quality wafers (with comparable efficiencies) without the need to saw ingots into individual wafers. The process is actually a two-part process of first creating a wafer, and with a subsequent step, improving its electrical properties. Shown in Figure 4 is a schematic of the initial wafer creation step. Molten silicon is poured onto a cool substrate and rapidly solidified into a wafer. The process is fast and cheap, resulting in a wafer that requires no post-process sawing or grinding. However, the wafer produced from the rapid solidification has very poor electrical properties. To improve these properties, including increasing grain size and decreasing dislocation density, a subsequent step is required.

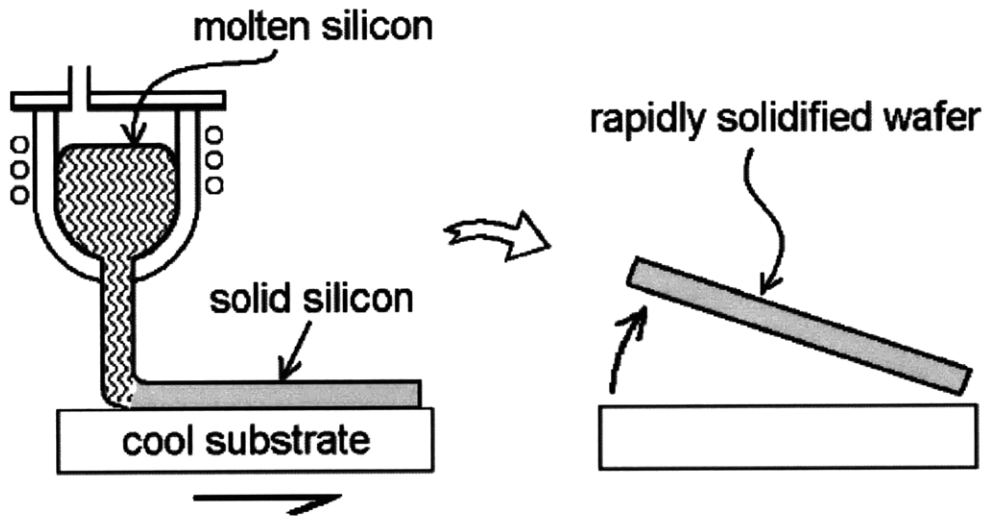


Figure 4: Schematic of the initial wafer creation process. Molten silicon is poured onto a cool substrate and rapidly solidified, producing a wafer with correct overall form but poor electrical properties.⁶

Following the creation of a rapidly solidified wafer, a step is needed to enhance electrical performance. This step requires zone melting and recrystallizing the wafer in a controlled manner. The wafer is placed between supporting material such as backing plates and sent under a series of heaters which melt the wafer as it passes through the furnace. Upon exiting the “hot zone,” the wafer is directionally cooled and solidified as shown in Figure 5. Done in a controlled manner, the recrystallization step seeks to increase grain size and reduce dislocation density to produce a wafer with comparable electrical properties to traditional cast-multi wafers.

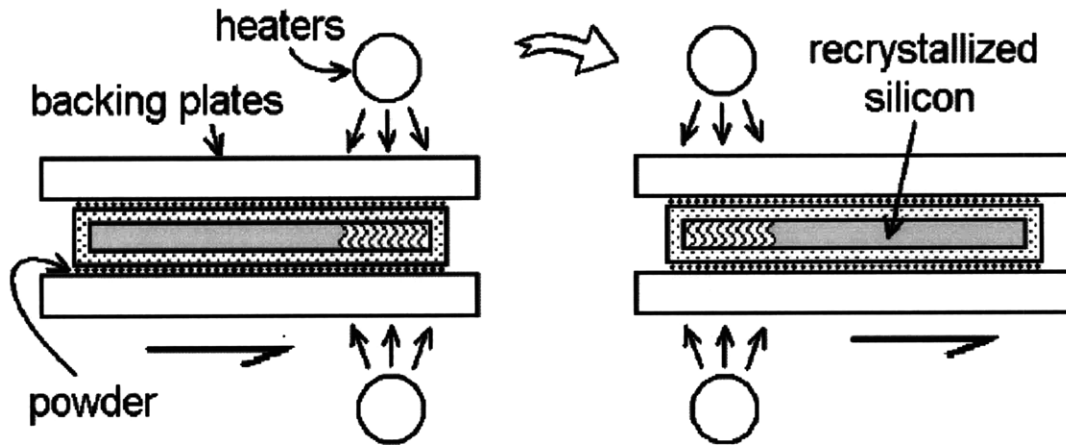


Figure 5: A schematic of the recrystallization step to improve the electrical properties of the rapidly solidified wafer. The wafer is zone melted and solidified in a controlled manner to improve electrical properties by increasing grain size and decreasing dislocation density.⁶

The overall goal of this process is to produce low-cost wafers with comparable electrical properties to that of cast-multi wafers. A critical cost-reduction method is to remove the post-processing sawing required for cast-multi wafers. The geometry of the wafer is defined during the initial rapid solidification. In a subsequent step, the wafer's electrical properties are refined. An important consideration in the subsequent recrystallization step is that the geometry of the wafer remains unchanged upon entering and exiting recrystallization, removing the need for post-processing alterations of geometry which are costly and wasteful.

To accomplish the main goal of removing the need for post-process sawing or grinding, it is imperative to maintain the geometry of the wafer during the recrystallization step. An important consideration during recrystallization is that all components exposed to the molten wafer must not present impurities to the wafer itself. Therefore great care must be taken in material selection for any structure designed to maintain wafer geometry as well as the components of the furnace itself. Additionally, the geometry and specifically the thickness of the wafer must conform to a given tolerance specification. Conventional cast-multi wafers have a maximum of 20 μm thickness variation, and that will be the goal of the output of the proposed process.

First, an oxide capsule is grown on the wafer by placing the wafer in a furnace at 1200 C for 20 hours. A layer of SiO₂ of slightly less than 1 μm envelopes the wafer to contain the molten silicon during recrystallization. The purpose of the oxide capsule is to contain the molten silicon during recrystallization. It was initially thought that the oxide capsule itself would provide a good structure for controlling the wafer's geometry when molten. However, the capsule provides very little support and behaves like a layer of plastic wrap, just containing the molten silicon and providing no structure. Photographs of a wafer recrystallized with an oxide capsule and no backing plates are shown in Figure 6.

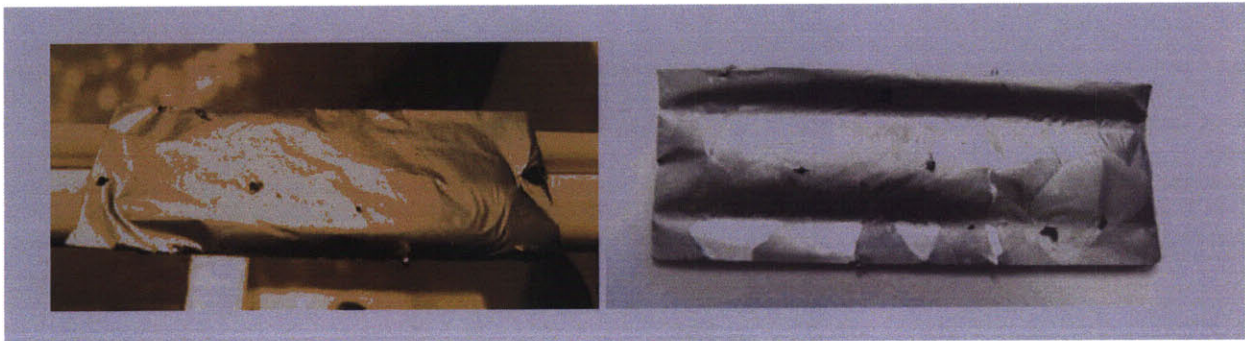


Figure 6: Photographs of a wafer that was recrystallized without backing plates. The oxide capsule grown on the wafer was sufficient to keep the molten silicon from falling off the guider bars. However, the oxide capsule did not provide enough structural support to prevent the wafer from deforming from its initial shape.⁶

The initial setup for the recrystallization process is shown in Figure 7 (and also displayed in Figure 5). The oxidized wafer is then placed between two silicon carbide backing plates, with a thin layer of silica powder separating the wafer from direct contact with the backing plates (to avoid the wafer adhering to the backing plates). Multiple methods of applying silica to the backing plates was tested, and powder-coating proved to provide a thin even coating. Silicon carbide and silica powder were chosen for their ability to within stand temperatures in excess of 1420 C, the melting point of silicon. Additionally, both materials (in their high-purity form) do not expose the wafer to impurities that may diffuse into the wafer at high temperatures and reduce electrical properties.

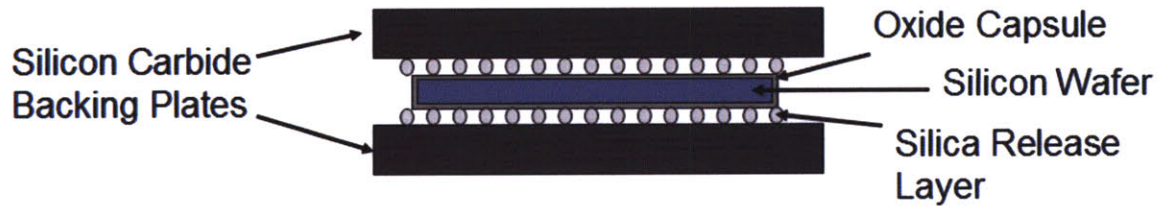


Figure 7: Preliminary recrystallization setup. An oxidized wafer is placed between two backing plates with a layer of silica powder to allow separation following recrystallization. The oxide capsule retains the molten wafer while the backing plates control the wafer's thickness as it is recrystallized.

1.3.1 Initial Results

The initial results for thickness control using two backing plates show that additional work is required to control thickness variation during recrystallization. With the amount of variation in wafer thickness present, post-processing would be necessary, bringing back waste streams and increasing the cost of the resultant wafers. Shown in Figure 8 is a photograph of a wafer recrystallized between two SiC backing plates. The wafer exhibits a wedge shape, whereas the leading edge is thin, and the thickness increases moving toward the trailing edge (in Figure 6 the right edge is the leading edge). The total thickness variation across the wafer is 212 μm , an extremely high number, and much too large for the goals of the recrystallization process. In addition to not preserving the thickness of a silicon wafer during recrystallization, parallel backing plates also do not preserve the horizontal geometry of a wafer. As can be seen in Figure 6, the trailing edge of the wafer is distorted with a large outward protrusion in the upper left corner.



Figure 8: Photograph of a wafer recrystallized with parallel backing plates. The right side of the photograph is the leading edge and the left side is the trailing edge. The non-uniformity on the trailing edge of the wafer displays how poorly parallel backing plates preserve the geometry of a wafer during recrystallization.

1.3.2 Proposed Method of Preserving Geometry

Our objective is to create a structure that will preserve the wafer geometry during recrystallization so that no post-processing is necessary. This will allow us to produce wafers with electrical properties on par with traditional cast-multi wafers, and at a much lower cost to the end user. A new direction, which is the bulk of this work, is depicted in Figure 9. The rapidly solidified wafer is placed on a silicon carbide backing plate and subsequently covered in powder. The combination of the backing plate and powder bed provides a shell that encases the wafer. When raised to sufficient temperature, the powder will sinter, creating a rigid shell that retains wafer geometry during recrystallization. The powder bed will initially conform to the shape of the incoming wafer. When sintered, the powder bed will create a rigid shell that will not allow silicon to translate or distort from its original shape. The main challenge of this proposed solution is in choosing a powder that will sinter and rigidly contain the wafer. The additional constraint that the powder must not present any impurities to the molten wafer further adds complexity to the solution.

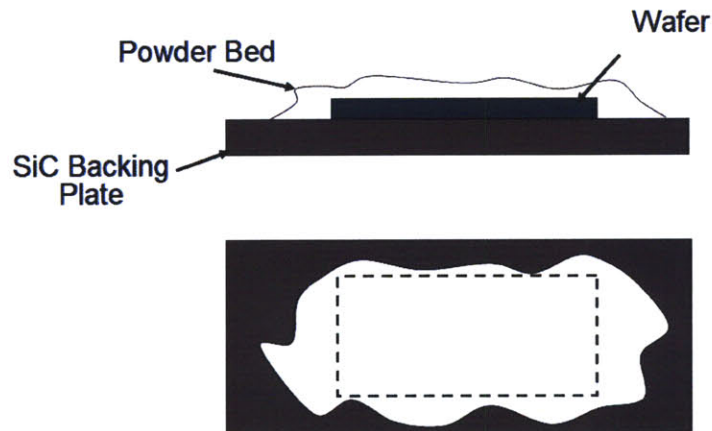


Figure 9: Schematic of new setup to control thickness variation during recrystallization step. The rapidly solidified wafer is placed on a silicon carbide backing plate and powder is placed on top of the wafer. The powder encases the wafer and when raised to sufficient temperature, it sinters, creating a rigid case that retains the wafer during recrystallization.

1.4 Powder Shell vs. Other Ideas

The idea of using powder to encase the wafer seems like a very complex solution to the problem. An easier way to encase the wafer would be by removing material in the shape of the wafer from either of the backing plates shown in the initial setup. This proposed setup is shown in Figure 10, and at first glance seems far superior to the powder shell technique. The backing plates need to be only created one time, and can be used for multiple recrystallization runs, as long as molten silicon does not stick to them. However, this method assumes that all incoming material is identical in its dimensions. In reality, the incoming wafers from the rapid solidification process will vary in size, and this method will only further increase that variation.



Figure 10: Schematic of setup where a portion of the top backing plate in the shape of the wafer is removed. A simpler solution than creating a sintered powder shell, but the technique does not account for variation of the incoming wafer.

Powder is an interesting substance that behaves to some degree like a viscous liquid. The main feature that makes it attractive for geometry preservation during recrystallization is its

ability to conform to its surroundings. Powder is placed on the wafer and backing plate and surrounds the wafer. The powder can then be sintered to form a rigid structure in the exact shape of the incoming wafer. Figure 11 is a schematic depicting the process of applying powder to the wafer and backing plate, having it contain the wafer during recrystallization, and finally separating the components and removing the recrystallized wafer.

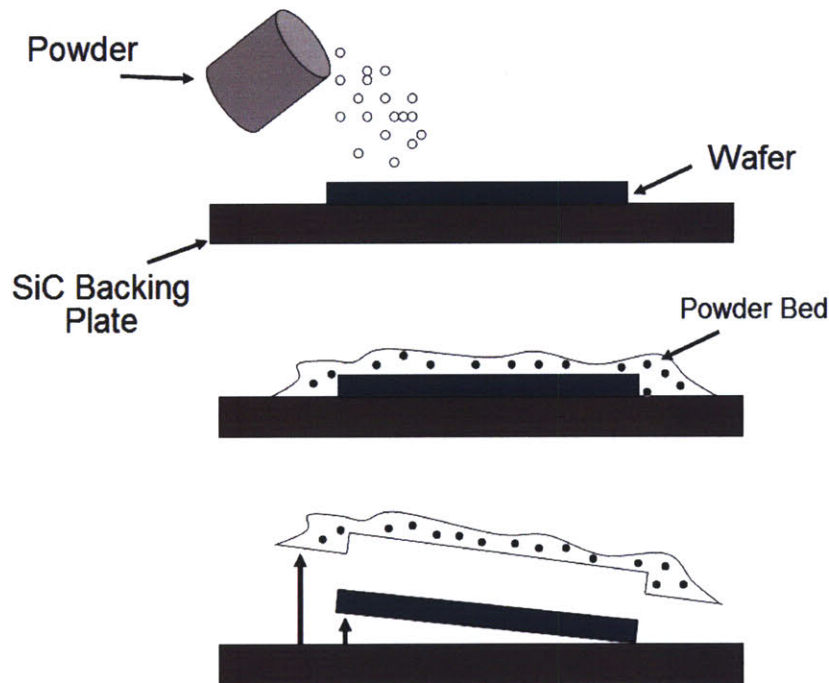


Figure 11: Schematic of the process for applying a powder to the wafer to preserve its geometry during recrystallization. Powder is poured over the backing plate and wafer, the shell contains the wafer during recrystallization, and the components are separated and the final wafer is removed.

1.4 Overview and Important Considerations of Powder Shell

Our objective is to create a shell that will contain the geometry of a silicon wafer during recrystallization. The proposed apparatus for controlling critical dimensions of a wafer during recrystallization is shown in Figure 12. Creating a powder shell may seem like it adds too much complexity to the problem than is actually necessary. However, powder actually adds flexibility because it allows for variation in the wafer exiting the rapid solidification process and entering the recrystallization step. Predefined structures do not offer this flexibility, actually creating more variation and complexity to geometry control during recrystallization.

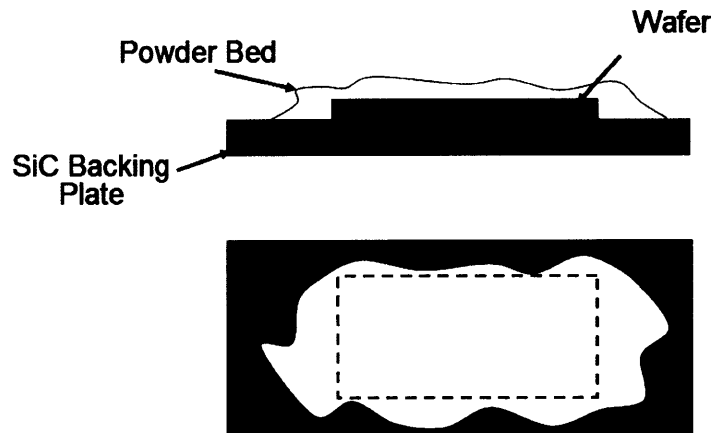


Figure 12: Schematic of proposed apparatus for controlling the critical dimensions of silicon wafer during recrystallization process. The wafer is placed on a silicon carbide backing plate and subsequently covered in powder. The powder and backing plate create a shell, encapsulating the wafer during recrystallization.

Before determining how to create a powder shell, it is first necessary to define what is needed of the structure to control a wafer's geometry. During the recrystallization step, the wafer transforms from solid to liquid phases and then back to solid during the final solidification step. In this transformation, it is important that the powder shell be an intact structure with no cracks or voids that would allow liquid to flow from the initial shape imprinted in the powder bed. Figure 13 shows a situation where there is a void in the powder shell that the molten silicon will flow into, resulting in the distortion of the final recrystallized wafer. A photograph of a wafer that was recrystallized in a powder shell that contained a void is shown in Figure 14. The elevated middle section is a result of a void in the powder shell and adds enormous variation in the thickness of the wafer. The shell must therefore be a perfect imprint of the initial wafer. To achieve this imprint, two considerations must be made. The powder must be placed on the top wafer and conform to the shape of the wafer. Additionally, the powder shell must remain intact and not distort or crack when sintered and subsequently when exposed to high temperatures during the actual recrystallization.

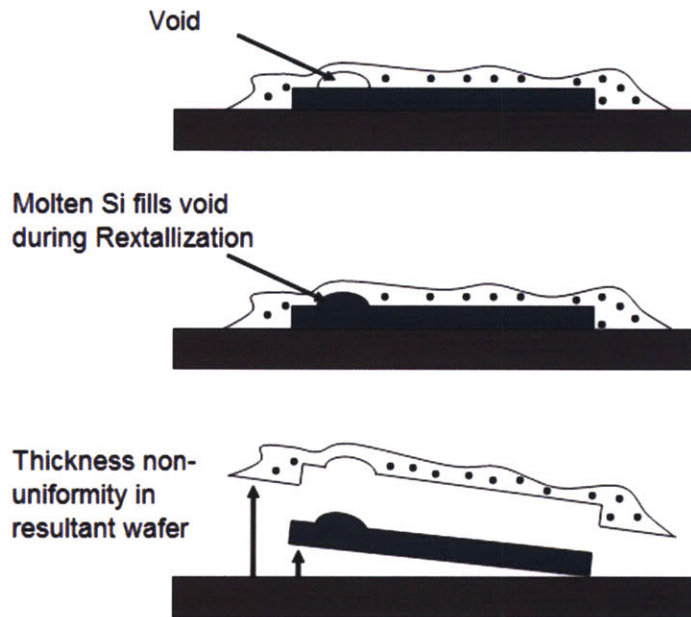


Figure 13: Schematic of case when a void is present in the powder shell. During recrystallization, molten silicon will flow freely into void space, resulting in immense thickness variation in the final wafer. In order to alleviate thickness non-uniformity, the powder shell must be free of voids and cracks during recrystallization.



Figure 14: Photograph of a wafer after being recrystallized with a powder shell. The hump across the center of the wafer is a result of a void present in the powder shell.

In addition to needing a uniform structure with a precise imprint of the recrystallized wafer, it is also necessary to have a rigid structure to encase the wafer during recrystallization. Silicon is an uncommon material in that it expands 10% when it freezes. The recrystallization process involves zone melting the silicon wafer resulting in a freeze front that propagates across the wafer. This freeze front is an important component of the process because it controls grain nucleation and growth, which determine the electrical performance of the wafer. However, although the traversing freeze front is important to improving the electrical properties of the

silicon, it provides challenges in the realm of geometry control. In particular, it dictates that a rigid structure is needed as opposed to a loose bed of powder. If a loose bed of powder were employed, the powder would drop from its original orientation as the wafer decreases in thickness upon melting. As the wafer travels through the furnace it would begin to freeze at the leading edge. This would result in a 10% volume expansion, causing the wafer's thickness to increase, putting an upward force on the layer of powder. This would result in either the powder cracking or deforming, and the geometry of the wafer would not be retained. Thus, there is a need for the rigid shell to maintain the original geometry of the wafer, allowing the wafer to contract and expand in volume without affecting the shell.

Finally, in addition to the above constraints, the powder must also be chosen so that it does not present impurities to the molten wafer. This limits our choice of powder to high-purity materials that can be exposed to the wafer at high temperatures and not effect the end electrical properties. Sintering a powder into a rigid shell from a short list of appropriate materials is not an exact science. The process of placing the powder on top of the wafer and backing plate so that no voids or imperfections is a difficult task. The process of then creating a rigid form of that powder bed also poses many challenges. Although there are rules and guidelines for creating a solid form by maximizing sintering, in the end, the optimal powder must be experimentally determined. The following context outlines our powder selection methodology and introduces theory for going about obtaining a rigid powder case.

Chapter 2

Powder Shell Capsule Technique

2.1 General Sintering Theory and Problems

The previous section is a detailed outline of what is precisely needed of the powder shell to retain geometry of silicon wafers during recrystallization. The following is a detailed description of how to achieve those objectives with use of powder sintering theory, and it identifies some key challenges that arise when sintering powder beds.

2.1.1 Sintering Basics

We must properly sinter the powder bed in order to create a rigid shell to encase the wafer. Generally speaking, sintering is the bonding of particles at high temperatures, typically at two-thirds the melting point of the material. In general, powders have high surface energies associated with them, and that energy is proportional to the specific surface area (area per unit volume). Powders made of smaller particles have higher specific surface area and surface energy and as a result, they sinter faster than larger particles. The powder wants to be at a state of lower energy, and over time it reduces its energy by reducing its specific surface area. Surface area reduction is obtained as neighboring particles join at contact points to form necks. Neck growth between two zinc particles is shown in Figure 15. This thermodynamic driving force toward a state of lower energy allows one to create a rigid structure from fine particles.⁷

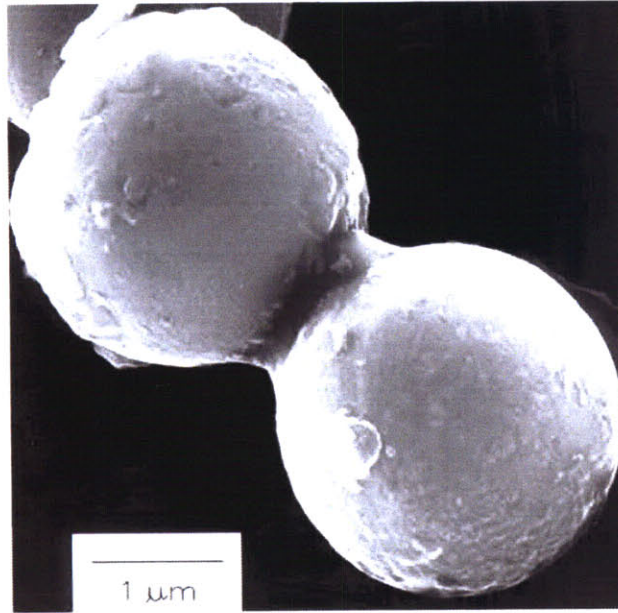


Figure 15: SEM micrograph showing the neck growth between two sintered Zn particles.⁸

In creating a shell that retains the wafer geometry, it is desirable to have a rigid shell as well as an intact shell that gives a good imprint of the initial wafer. To create a rigid shell, it is desired to maximize the amount of sintering that takes place. As stated above, smaller particles with greater specific surface area sinter better than larger particles. Sintering time also impacts the degree of sintering. Figure 16 shows the evolution of powder sintering over time. The longer a powder is held at an elevated temperature, the more sintering occurs, and the denser it becomes, creating a more rigid, structurally sound shell. However, it is important to consider that as well as providing a rigid structure, we must also create a uniform, intact structure that maintains the initial imprint of the wafer.

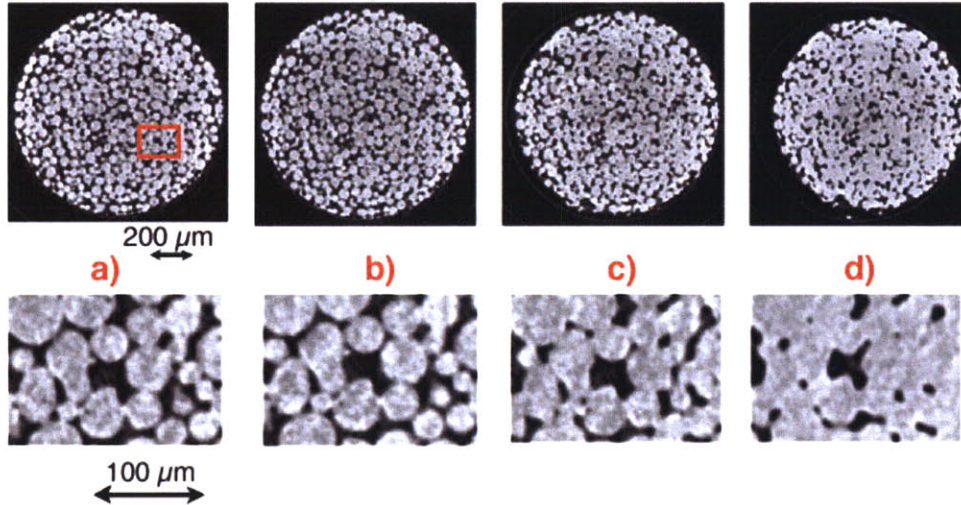


Figure 16: Shows the evolution of powder sintering over time. As time increases, powder particles join more successfully, creating a denser structure. Over time, as the particles sinter more and more, less void space is apparent in the bulk of the material.⁹

2.1.2 Shrinkage and Voids

Shrinkage is an important problem in powder sintering. As a powder bed sinters, particles begin to join together, removing the void space that was once present (displayed in Figure 16). As void space disappears, shrinkage of the total space that is occupied by the powder bed occurs. The density of the actual powder remains unchanged, but the density of the entire powder *bed* becomes greater (as the dimensions of the bed become smaller). Because all sintering processes involve particles joining, shrinkage is almost always an unavoidable side-effect when sintering. Although it is unavoidable, the *amount* of shrinkage is controllable. The initial density and porosity of a powder bed has a large effect on the amount of shrinkage that occurs during sintering. A more porous powder with a lower density will tend to shrink more than a powder with less void space. Additionally, the amount of sintering (dependent on the total sintering time and sintering temperature) affects the amount of shrinkage of a powder bed. Figure 17 is a graphical representation of the effects of sintering time and temperature on the shrinkage of a powder bed. The amount of shrinkage is proportional to both the sintering time and sintering temperature; to decrease shrinkage, one must decrease time and temperature.

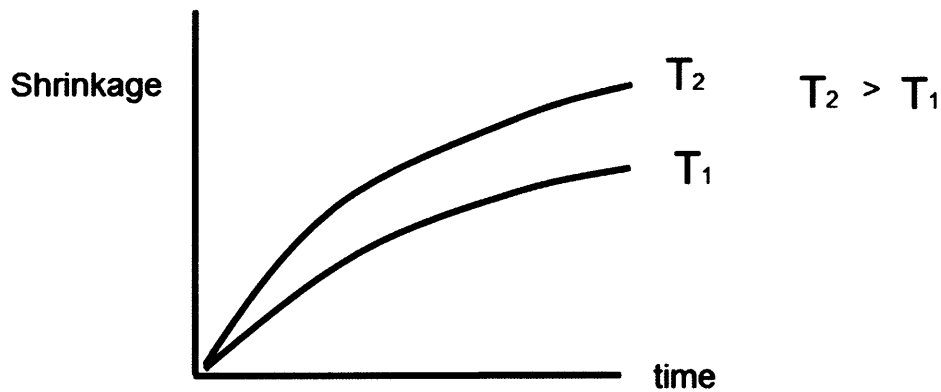


Figure 17: Graphical depiction of the effects of sintering time and sintering temperature on the shrinkage of a powder bed.⁷

Voids are another problem in powder sintering. A void in the powder bed and resulting shell would allow liquid silicon to flow out of its initial shape and recrystallize in a distorted fashion (as shown in Figures 13 and 14). A void is effectively a hole in the powder bed and is a result of improper settling of individual particles. Voids or pores in a powder structure result in a structure with a lower density than is maximally achievable. Explained in the following section, powder compaction is a process of decreasing porosity and voids and increasing density of the powder bed.

2.2 Methods of Improving Sintering

Sintering powder into a rigid shell with a very fine tolerance range provides many challenges. From shrinkage to voids and cracks in the powder bed, the challenges are difficult, but there are measures to take to alleviate them. The following is an in depth theoretical analysis of methods for improving a powder shell for geometry control during the silicon recrystallization process. It includes guidelines for increasing sintering and reducing geometrical change in powders while they are raised to elevated temperatures.

2.2.1 Compaction: Reducing Voids and Increasing Packing Density

Voids or pores in a powder structure result in a structure with a lower density than is maximally achievable. Compressing a powder before sintering reduces porosity and voids, and increases the packing density of a powder bed. Compaction reduces shrinkage by reducing the

porosity in the powder bed. Overall, compaction increases the “strength, density, shape definition, and dimensional control,” in the creation of a structure using powder sintering.⁷ In general there are three methods of powder compaction: physical compaction, vibrational compaction and slurry-casting compaction.

Physical Compaction

The most common type of powder compaction is physical compaction which is performed by applying pressure along one axis to a powder bed with hard tools. A diagram depicting physical compaction is shown in Figure 18. Physical compaction is not a good choice for this application because of the frailty of the silicon wafers. Wafers tested were on the order of 200 um thick. Physical pressure placed on the wafer could cause them to crack, lowering the yield of the process and producing an extra, undesirable waste stream.

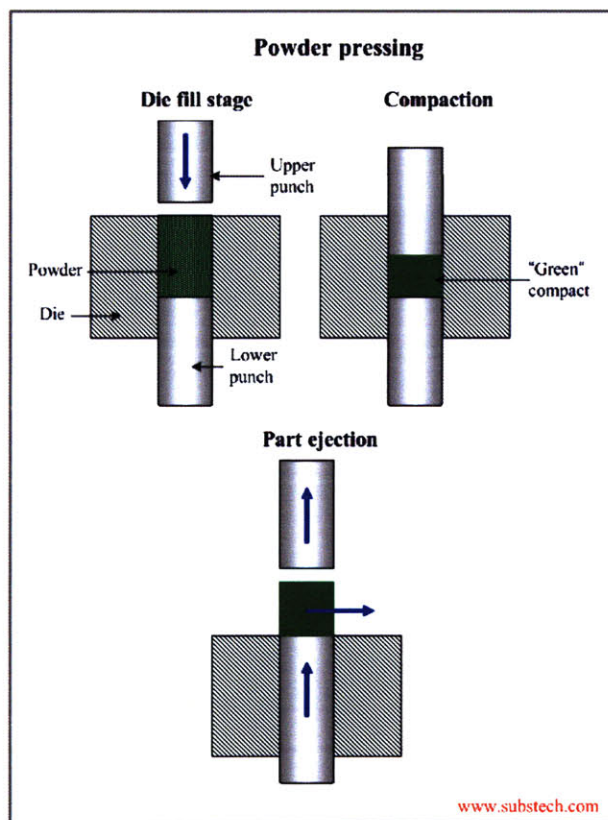
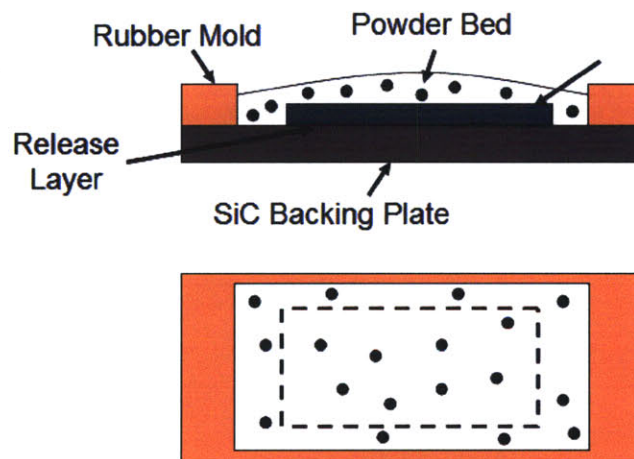


Figure 18: Schematic of the most common form of powder compaction: physical compaction. Loose powder is placed between two punches as they are forced together, pressing the powder into a “green” compact. This process provides a great green compact, but is undesirable in our process as it could result in the wafer cracking.¹⁰

Vibrational Compaction

A diagram depicting vibrational compaction is shown in Figure 19. Dry powder is poured into a mold on top of a wafer and backing plate. The entire apparatus is then vertically vibrated to densify the powder bed and to cause the powder to better surround the wafer (while eliminating void space). Powders are initially poured and friction between particles cause them to not pack to their maximum potential. The mechanism behind vibrational compaction is that as vibration occurs, particles are allowed to freefall, gaining momentum to pack together in a more compact, orderly fashion. Imagine a giant pool filled with golf balls. The balls will not necessarily be in a perfect arrangement, but will rather contain voids and empty space. Now raise that pool and drop it, allowing the balls to freefall before crashing to the bottom. With the momentum built from freefall, the balls will fill void space and create a more compact final arrangement. Vibrational compaction does provide some densification, and it is advantageous for the recrystallization step because it is a dry process. Therefore, it will not destroy or disturb the silica release layer, allowing the wafer to be removed following recrystallization.

Vibrational Compacting



Dry process.

Figure 19: Schematic of a powder shell created by pouring a dry powder mixture over the wafer and backing plate. A rubber mold is placed onto of the backing plate surrounding the wafer to contain the powder and prevent it from falling off the plate. Powder is placed within the mold and the entire apparatus is vibrated, to allow powder particles to line up properly and fill the space on top of the wafer. An advantage of this process is that it is dry and would not disturb the release layer between the wafer and plate.

Slurry Compaction

In terms of the amount of compaction that it provides, slurry compaction is a superior technique to vibrational compaction. However, slurry compaction is a wet process, which is disadvantageous in the recrystallization process. Liquid from the slurry has the ability to flow between the wafer and backing plate, disturbing the release layer and resulting in the wafer being stuck to the backing plate following recrystallization.

Figure 20 is a schematic of a powder shell created by the slurry casting technique. Powder is first mixed with a liquid depending on the desired amount of viscosity (can mix with water or alcohols). The resultant slurry is then poured on the wafer/backing plate within the mold and allowed to dry. The liquid in the slurry acts as a lubricant between particles, allowing them to slip past each other to compact nicely over the wafer. This reduces the number of voids in the powder bed and increases its overall density. However, slurry casting is not an ideal method of compaction because liquid can flow underneath the wafer, disturbing the release layer and enabling the wafer to stick to the backing plate.

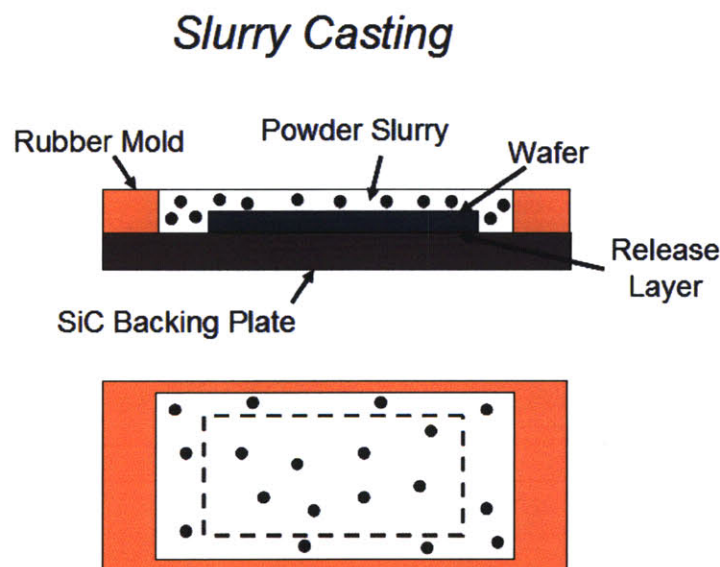


Figure 20: Schematic of a powder shell created by pouring a liquid-powder mixture (slurry) over the wafer and backing plate. A rubber mold is placed onto of the backing plate surrounding the wafer. The slurry is then poured into the mold, creating a compact layer of powder over the wafer. Slurry casting provides a far superior compaction than vibration compaction. However, it is a wet process that results in slurry flowing underneath the wafer, disturbing the release layer, and allowing the wafer to stick to the backing plate during recrystallization.

2.2.2 Bimodal Powders

Bimodal powders are a mixture of two different particle sizes and have some benefits over traditional powders. Traditional powders with a quoted particle size are a powder mixture with a monomodal distribution. Although an average size is quoted, the powder is actually a distribution of different sized particles that have a mean particle size and standard deviation. All commercial powders have some distribution associated with their particle size, giving a range of actual powders. Bimodal powders are a blend of two monomodal distributions and have the ability to enhance some properties of the overall powder mixture. Shown in Figure 21 is a diagram comparing monomodal and bimodal powder mixtures.

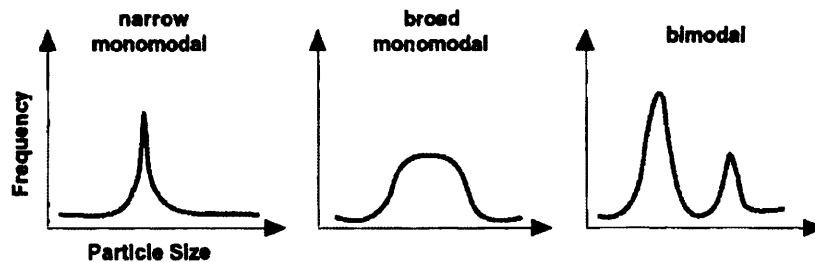


Figure 21: Three graphs displaying different types of powder distributions. The left-most graph is a narrow monomodal distribution in which there is a small standard deviation amongst particle sizes. The middle graph shows a broad monomodal distribution which has a wide range of particle sizes (large std. dev.). Finally, the right graph shows a bimodal distribution which is a mixture of two monomodal distributions.¹¹

A bimodal powder is a combination of two monomodal powders with different mean particle sizes. With a monomodal powder, the maximum obtainable packing density is 64% (meaning that 36% of the space of the powder bed will be empty). However, with a bimodal powder, it is possible to achieve a packing density of 75-80%. Figure 22 is a schematic depicting the bimodal packing concept. The idea behind bimodal packing is that smaller particles fill the void space between large particles. This occurs without forcing larger particles apart, resulting in a higher density because void space is now being filled with particles. Mixing any two powders of different particle sizes does not guarantee an increase in green density. Important factors which affect the green density of a bimodal mixture are the volume ratio of

small particles to large particle and the ratio between the diameter of small particles to the diameter of large particles.¹¹

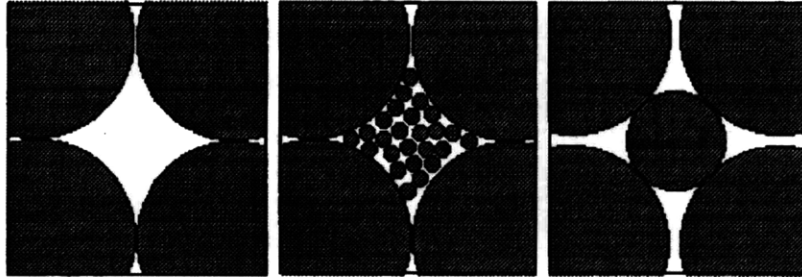


Figure 22: Schematic of bimodal packing. Smaller particles fill the void space between larger particles, increasing the packing density and therefore, the sintering rate.¹¹

The ratio of diameters of small particles to large particles is an important factor in determining the packing density of the bimodal mixture. Ideally, the ratio of diameters would be as large as possible to allow smaller particles to easily fill the interstitial space between large particles. As shown in Figure 21, as the diameter of the smaller particle approaches that of the larger particle, the benefit of the bimodal mixture begins to get lost. Shown in Figure 23 is a plot of diameter ratio ($D_{\text{Large}} / D_{\text{Small}}$) versus packing density.

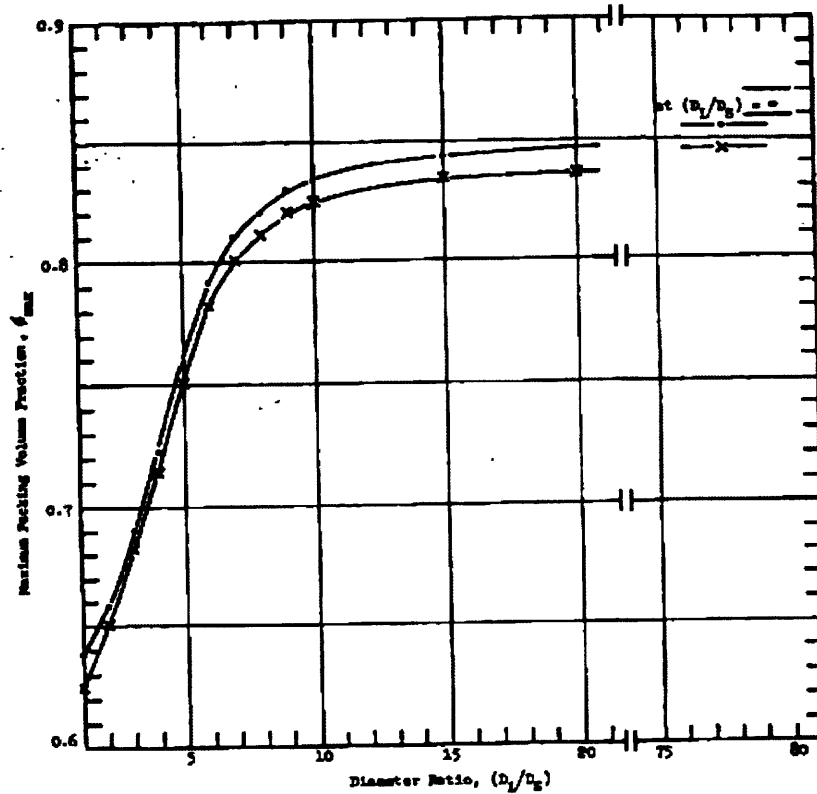


Figure 23: Plot of diameter ratio (D_{Large} / D_{Small}) versus packing density for a bimodal mixture. In general, the larger the diameter ratio between large and small particles, the better the packing density of the bimodal mixture. However, examining the graph closer, the benefit of increasing the diameter ratio diminishes as the graph flattens out at a ratio of 10:1 (D_{Large} / D_{Small}).¹¹

The volume fraction of small particles to large particles is another important factor that determines the packing density of a bimodal mixture. Figure 24 is a plot showing the relationship between the volume fraction of large particles to small particles and the packing density of the bimodal mixture. The various lines in the plot correspond to different diameter ratios of small to large particles. For every diameter ratio, the maximum packing density is achieved at 73.5% large particles and 26.5% small particles. Also, we can observe from the graph that the packing density diminishes more rapidly if the volume fraction of large particles is increased beyond 73.5%. Therefore, in all cases it is better to have an excess of fine particles rather than large particles.¹¹

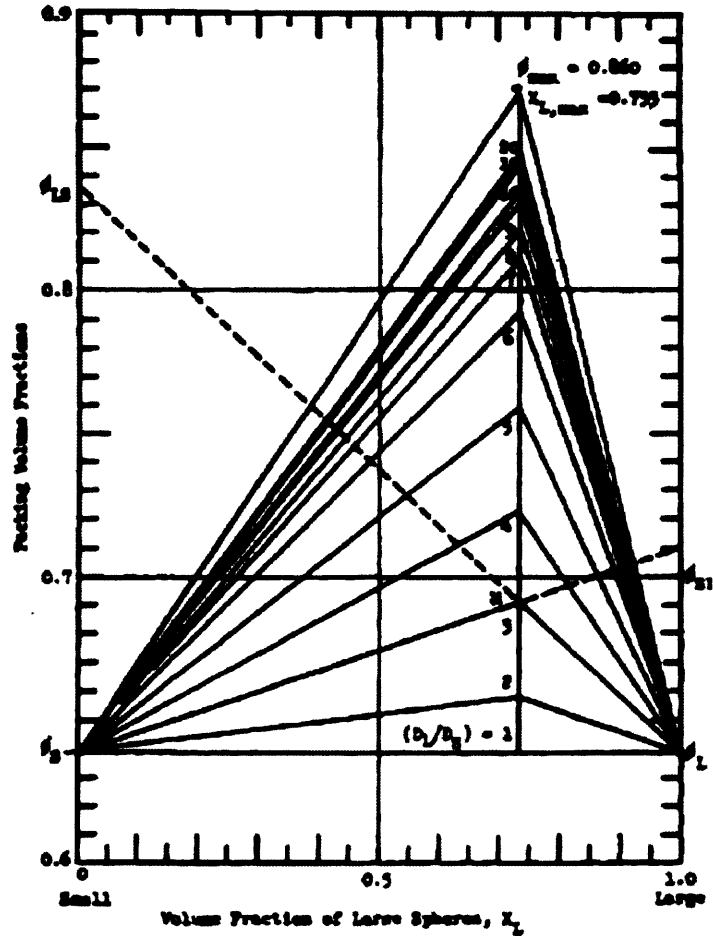


Figure 24: Plot showing the relationship between the volume fraction of large particles to small particles and the packing density of the bimodal mixture. The different lines in the plot correspond to different diameter ratios of small to large particles. For every diameter ratio, the maximum packing density is achieved at 73.5% large particles and 26.5% small particles.¹¹

Overall, the diameter ratio and volume fraction of small particles to large particles are two important factors that determine the packing density (and therefore sintering ability) of a bimodal powder mixture. The optimal diameter ratio of large particles to small particles is greater than 10:1. The optimal volume fraction of large particles to small particles is 73.5% large particles regardless of the diameter ratio. It is also important to note that in all cases, it is more desirable to have an excess of small particles than large particles. These two guidelines can be used to govern the creation of a powder shell using bimodal powder mixtures.

2.3 Proposed Process for Recrystallization

2.3.1 Powder Selection

Appendix A is a detailed overview of the powder selection process. It outlines the multiple powders that were tested and the methodology behind choosing an appropriate powder for the recrystallization process. After extensive tests, the final powder chosen for use in recrystallization was a silicon carbide bimodal powder. The powder is a mixture of 44 μm SiC powder and 2.5 μm SiC powder. The two powders were mixed with a volume ratio of 2.5:1 (small particles to large particles). The powder was mixed with an electric coffee grinder to ensure good mixing and to loosen any agglomeration that occurred within the mixture.

2.3.2 Powder Shell Creation Process

With an appropriate powder selected, it was now possible to recrystallize a wafer and determine how well the shell technique would control geometry of a wafer. To begin, 200 μm thick wafers are cut into 20 x 40 mm rectangles. The rectangular wafer is cleaned and prepped to enter the oxidation furnace. The wafer is placed into a tube furnace at 1100 C for 20 hours to grow an oxide layer slightly less than 1 μm thick.

A high-purity Hexoloy SiC backing plates (3.5" x 1.5") is used to support the wafer during recrystallization. The plates are very resistant to corrosion and deformation at high temperatures, and are pure, introducing no impurities to the molten wafer during recrystallization. The backing plate is then lightly powder coated with coarse silica powder (40 μm) to act as a release layer between the wafer and plate. With the coating in place, the oxidized wafer is placed on the coated backing plate carefully, to not disturb the release layer. With the wafer in place, a silicone rubber mold is placed on the backing plate, leaving room around the wafer for the powder bed. The mold is now set and ready to be filled with powder. The SiC bimodal powder mixture is poured within the mold on top of the wafer slowly, to ensure not to disturb the wafer and release layer. With the powder in place, the entire apparatus is then vibrationally compacted to remove voids and increase the packing density of the powder. This is done by striking the entire apparatus multiple times on the table top until the powder's top surface becomes smooth. A photograph of the compacted powder shell within a silicone rubber mold is shown in Figure 25.



Figure 25: Photograph of the recrystallization setup after powder has been poured over the wafer and vibrationally compacted. The rubber mold keeps the powder from spilling off of the backing plate. The powder bed is not a perfect layer, but is an improvement over the initial state of it after is been poured onto the wafer.

The set up is now complete, and the silicone rubber mold is removed from the backing plate. The backing plate, covered by the wafer and powder layer, are now placed into a box furnace at 1200 C for one hour. The purpose of this is to rigidize the powder layer before sending the entire package through the recrystallization furnace. Once the powder is sintered, the entire apparatus is sent through the recrystallization furnace build by Eerik Hantsoo. A photograph of the furnace is shown in Figure 26. A unique feature of the furnace is that it is composed entirely of high-purity materials, so to not contaminate wafers during recrystallization. The furnace is capable of reaching temperatures in excess of the melting point of silicon, and has three heating zones, each controlled separately by pyrometers. The backing plate with wafer and powder bed is placed on two SiC rods that move through the furnace. The heating elements are set to 1650 C and the package is run through the furnace at 9 mm/sec. These two parameters were experimentally determined by myself and Eerik Hantsoo as appropriate conditions for recrystallizing a wafer.

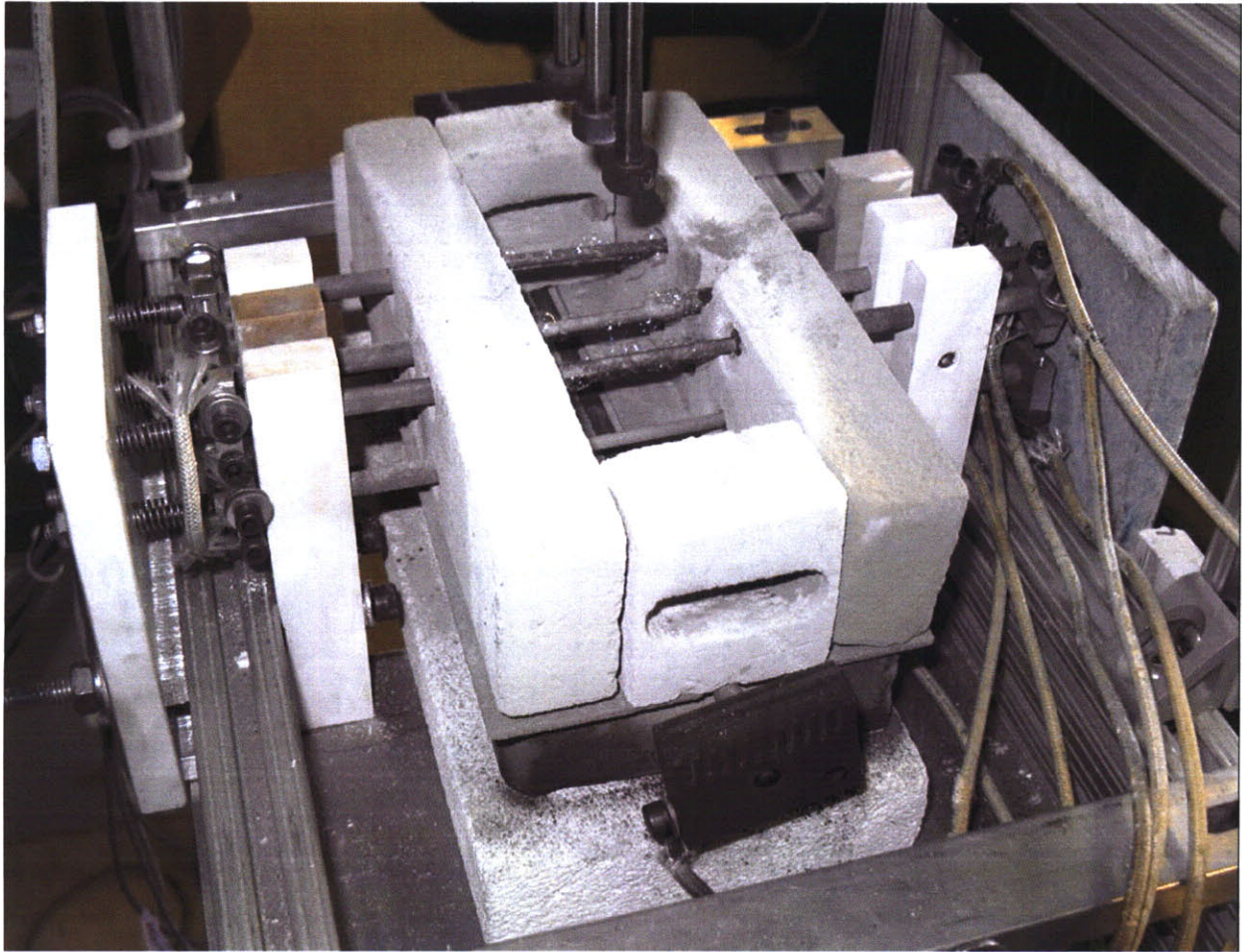


Figure 26: Photograph of the recrystallization furnace built by Eerik Hantsoo with help from Jim Serdy.

Following recrystallization, the wafer is removed from the powder shell and etched in hydrofluoric acid to remove any powder that adhered to it. The final clean wafer is then measured and analyzed to determine how well its geometry was preserved in the process.

Chapter 3

Ceramic-Coating Technique

3.1 Current Technique and Sand Casting

Our current process of creating a powder shell to encase the wafer during recrystallization is very similar to sand-casting used to create metal shapes. In sand casting, a mold is created in a bed of sand using a pattern of the desired final part shape. The bottom and top half of the part are created in two different sand beds and joined to create a mold in the desired shape of the mold. After creating a single mold in the shape of the desired part, molten metal is poured into the cavity and cooled, creating the final metal part.

Although we are not creating a mold with which to pour molten silicon, we are creating a similar structure to the sand mold for retaining a wafer's geometry during recrystallization. The process is identical to that of sand casting in that we are creating a mold using a pattern that is in the desired shape of the final part. In our case, however, the pattern itself remains within the mold and is melted and solidified rather than a molten material being poured into an empty cavity.

A big disadvantage of sand casting is that it is not a precise technique and usually produces parts with a high level of variation. This is highly undesirable during recrystallization as variation even in the micron range is unacceptable. Additionally, sand-casting also produces parts with poor surface finish due to the coarseness of the sand used. Such disadvantages of the process require post process machining and grinding in most-cases to achieve parts of acceptable dimensions. This is not acceptable as the purpose of the recrystallization process is to reduce waste streams by eliminating post-processing. Figure 27 shows indentations in a wafer that was recrystallized in a powder bed. The rough surface texture is due to the roughness of the powder bed and the surface finish is similar to a metal part created by sand casting.



Figure 27: Photograph of the bottom surface of a wafer following recrystallization within a SiC powder shell. The left edge of the wafer is the leading edge. The wafer has a very rough surface finish with frequent pits due to powder particles in contact with the wafer itself.

Although most of the above difficulties can be alleviated by choosing finer sand mixtures, it is also important to consider the compaction of the sand mold in the sand-casting process. Because the original pattern is usually a metal part that can handle intense stress, sand is physically compacted with immense pressure. This creates a mold in the shape of the initial pattern with few if any voids. This compaction is not transferable to our process because the pattern is a fragile, brittle piece of ultra-thin silicon. Other methods must be employed to compact the pattern, most of which do not fully remove voids.

With these clear disadvantages present, we decided to consider placing an interface between the powder bed and wafer so that the rough powder would not be in direct contact with the surface of the wafer. This could be achieved by coating the wafer in a ceramic slurry, that would create a rigid and durable interface (capable of withstanding high temperatures and stresses) between the wafer and powder bed.

3.2 Proposed Process for Recrystallization

The idea of coating the wafer in a ceramic slurry is loosely related to lost-foam casting. With the goal to create an interface between the wafer and powder shell, we designed a process to retain the silicon wafer's geometry during recrystallization. The basic process involves coating the wafer in a slurry of fine particles and then creating a powder shell much like the previous process.

A preliminary step in the process is creating a slurry with silicon carbide powder. Although different slurry compositions were tested, the original slurry was composed of a mixture of 2 μm SiC powder and 2 μm silicon dioxide particles. Water is the base of the slurry, and a thin layer is applied to the wafer using a spin-coating technique. The thin layer is dried and then fired in a furnace to 1200 C. This firing sinters the particles, creating a solid shell encasing the wafer. A photograph of the wafer coated in the SiC slurry is shown in Figure 28. It is important to note the edge effects that are a result of spin-coating the slurry onto the wafer. These edge effects result in distorted edges on the final recrystallized wafer.

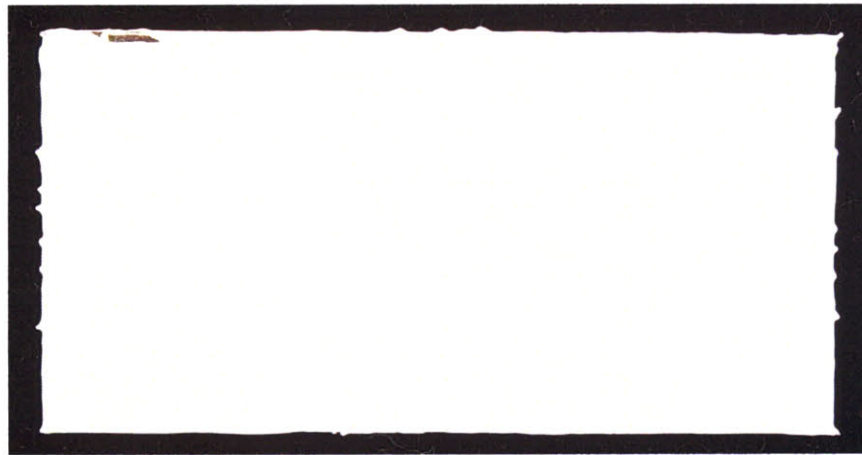


Figure 28: Photograph of a wafer with a spun-on coating of the oxidized SiC slurry.

After the slurry coating is in place, the original powder shell technique is applied to the coated wafer. The coated wafer is placed on a SiC backing plate and a powder bed is placed on top and then vibrationally compacted. A schematic of the entire package is shown in Figure 29. Once the setup is complete, the package is sent through the recrystallization furnace, where the slurry coating and powder backing retain the geometry of the wafer during the change from solid to liquid phases. Following recrystallization, the slurry coating is removed from the wafer by etching in concentrated Hydrofluoric Acid.

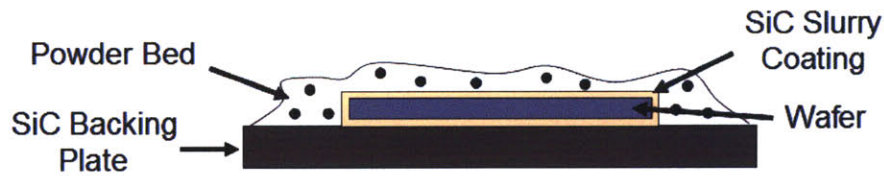


Figure 29: Schematic of the ceramic coating method of preserving geometry during recrystallization. The coating creates a rigid, smooth interface between the powder bed and wafer.

Chapter 4

Measuring Thickness Uniformity

Measuring the thickness uniformity of a recrystallized wafer is a difficult task given the desired maximum thickness variation of approximately 20 μm . Instruments such as thickness gauges and micrometers are often not accurate enough to measure micron-level discrepancies. Hand measurement involves taking measurements at different areas on the wafer to get an idea of thickness variation. From these measurements one can determine the thickness range across the wafer and other quantities that could characterize thickness variation. However, rather than simply finding the range of thicknesses across the wafer, it would be beneficial to generate a thickness map of the recrystallized wafer. A picture would allow us to closely examine what kind of thickness variation is present in the wafer. The physical picture of the wafer would additionally provide valuable information on how to correct any problems during recrystallization. The final component to measuring the thickness variation of a sample is the amount of time it takes to measure a sample. It is possible to create a thickness map with hand measurements but it would be extremely time consuming. Thus, it is desired to create such a picture in a short time without the need for extensive hand measurements or computation time.

Prior to developing the thickness measurement technique, wafers were measured by hand using a digital thickness gauge with 10 μm accuracy. The wafer was schematically divided into six sections for simplicity (shown in Figure 30), and the average thickness was determined with

measurements in each section. These six average thicknesses were compared, giving a crude measure of the thickness variation across a recrystallized wafer.

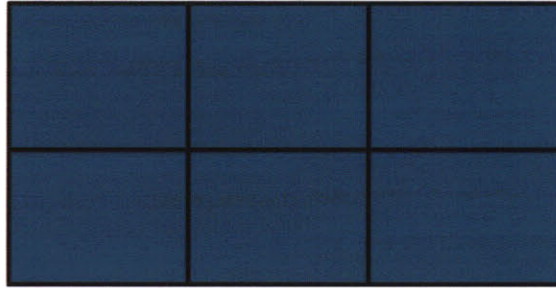


Figure 30: Diagram depicting how a wafer was divided to roughly quantify its thickness variation. Five measurements were taken in each of the six small rectangles, and the average thickness was found in each section. This was the initial method of determining thickness uniformity.

4.1 Beer's Law: Relating Thickness and Transmission

Silicon is used for solar cells and other photovoltaic devices because of its ability to absorb light. Silicon's absorption capability can also be used to determine its thickness. The relationship between the amount of radiation absorbed and the specific properties of the material is given by the Beer-Lambert Law (or Beer's Law). A schematic of Beer's Law is shown in Figure 31. Beer's Law states that there is a logarithmic relationship between the amount of radiation that passes through a material (the transmission) and the thickness of the material. It is given by:

$$I_1 = I_0 e^{-t\alpha} \quad (1)$$

where I_1 is the transmitted radiation, I_0 is the incident radiation, t is the thickness of the material, and α is the absorption coefficient. The absorption coefficient is not only specific to a given material, but also depends on the wavelength of the incident radiation.

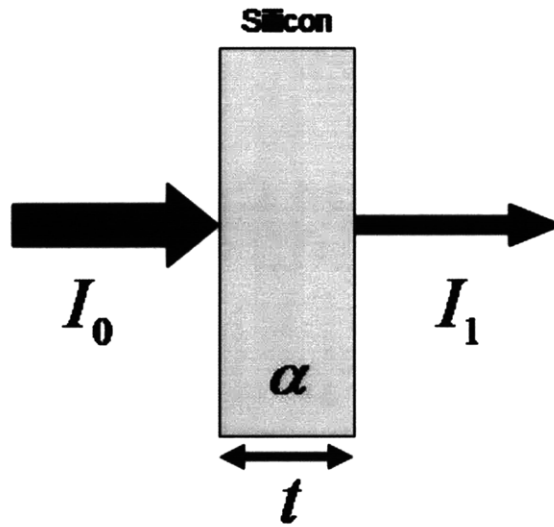


Figure 31: Diagram depicting incident radiation being absorbed by silicon of a given thickness, t . Beer's law explains that there is a logarithmic relationship between the incident radiation, I_0 , and the transmission, I_1 .

It is also important to consider that some radiation is lost to reflection as it passes through an interface separating two different materials. Figure 32 illustrates how a portion of the incident radiation is reflected as it strikes surfaces of the sample.

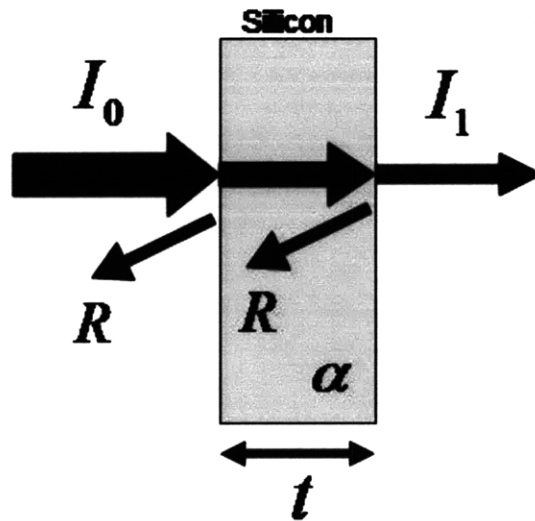


Figure 32: Schematic of radiation traveling through a piece of silicon of given thickness t . Light is absorbed as it travels through the silicon and it also gets reflected at each surface where the index of refraction changes. The radiation gets reflected when it first enters the wafer and subsequently when it leaves the back surface and returns to traveling in air.

At each interface, a fraction of the incident radiation, R , is reflected, diminishing the amount of light that is transmitted through the sample. The transmission is now reduced by a factor, $(1 - R)^2$, due to the existence of the two such interfaces that incident radiation strikes during its travel through the sample. The light that reflects off of the back surface of the wafer will bounce back and a portion of the reflected will get pass back through the wafer. However, this higher order term can be neglected in this analysis. The amount of radiation lost due to reflection depends on the indexes of refraction of two materials and is given by:

$$R = \frac{(n_1 - n_2)^2}{(n_1 + n_2)^2}, \quad (2)$$

where n_1 and n_2 are refractive indices of each material. Combining equations 1 and 2, and solving for thickness, the relationship between the thickness of a material and the transmission of incident radiation is given by:

$$t = \frac{\ln(I_0(1 - R)^2) - \ln(I_1)}{\alpha}. \quad (3)$$

Overall, according to Beer's Law, the thickness of a silicon wafer can be determined if the following parameters are known: the intensity of incident radiation, the transmission, the reflection coefficient, and the absorption coefficient. It is important to note that both α and R are highly dependent on the wavelength of the incident radiation.

4.2 Thickness Measuring Apparatus

Beer's Law can be used to generate a thickness map of a given silicon wafer. A schematic of the setup is shown in Figure 33. The apparatus includes an infrared light source, two diffusers, the wafer to be measured, and a CCD camera with an attached interference filter. The CCD camera is focused on the sample wafer while an infrared light source illuminates the wafer from behind. The light travels through the wafer and some portion is absorbed by the wafer in accordance with Beer's Law. The camera captures the intensity of light that is transmitted through the wafer.

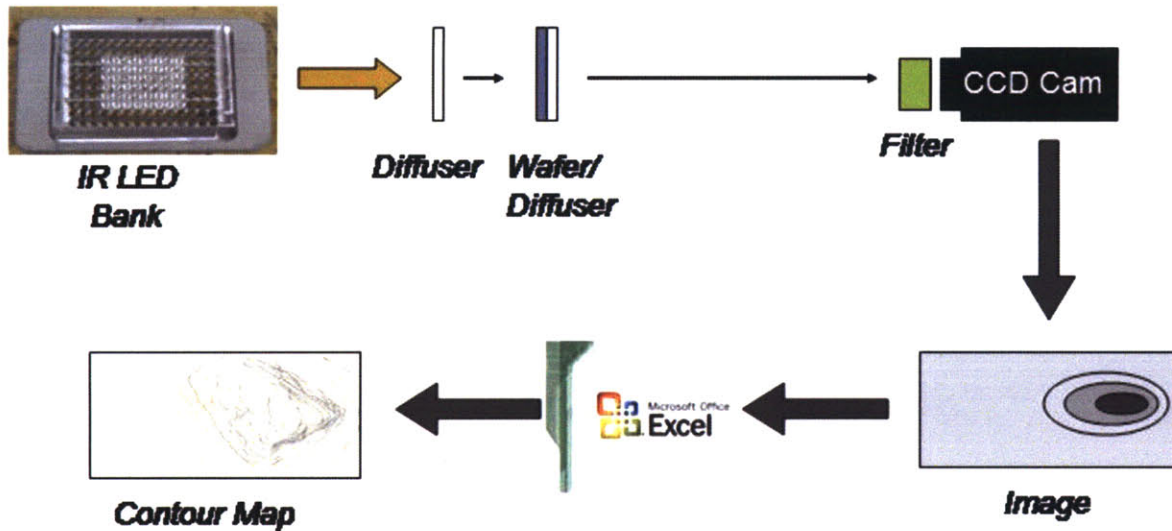


Figure 33: Diagram of the apparatus used to create a thickness map of a recrystallized wafer. Infrared light is projected through a diffuser and subsequently through a wafer. The light then passes through another diffuser and an interference filter where it is then captured by a CCD camera. The image from the camera is then analyzed and a contour map of the wafer is generated.

The purpose of using an IR light source is to provide incident radiation of a specific wavelength, which in turn provides theoretical values of R and α (both of which are dependent on wavelength). Infrared LEDs of 940 nm were specifically chosen because that wavelength provides adequate visual contrast when projected through a wafer in the 200 μm thickness range. Longer wavelengths would not be absorbed by the wafer, and shorter wavelengths would not display enough contrast between thicknesses to provide an accurate thickness map. It is important to note that although the majority of light emitted from the LEDs wavelength of 940 nm, the actual emission is a distribution of various wavelengths. To narrow the distribution of emitted light even further, a 940 nm interference filter is placed directly in front of the CCD camera (shown in Figure 30).

Between the wafer and the IR light source is a 15° holographic diffuser that blends the LEDs into a single source. Because the light source is an array of small, individual light sources, it is necessary to blend these sources to create a single, uniform light source. The holographic diffuser diffuses incident light in a conic fashion, allowing us to control the specific spot size of the incident light. This allows us to blend the individual radiation from each LED and not lose much intensity in the process.

The final important piece of apparatus is the diffuser placed between the wafer and the CCD camera. The path that light will take upon exiting the wafer is highly dependent on the

surface geometry of the backside of the wafer. Rough geometry on the surface will scatter light and result in brightness variation that is not a result of thickness variation. A standard ground glass diffuser is placed in direct contact with the wafer. This captures light directly leaving the wafer, removing the scattering effect caused by surface roughness. Overall, the diffuser allows us to capture the variation of light intensity caused solely by the variation in thickness across the wafer.

With a proper image recorded, it is necessary to process the image to generate a thickness map of a wafer. The image from the camera is first converted to grayscale in JPEG format so that each pixel is given a value of brightness. Once converted, the image is then sent to MatLab where each pixel is given a numeric value of brightness ranging from 0 (complete black) to 255 (complete white). The grid of pixel values is sent to Excel where the thickness map is generated using equation (3).

4.3 Measurement Calibration

It would appear from equation (3) that there are zero unknowns in the relationship between thickness and transmission. However, there are two parameters that must be experimentally determined. I_0 , the amount of incident radiation, and α , the absorption coefficient, both must be determined experimentally to produce an accurate relationship between thickness and transmission. It would make sense that I_0 would simply be 255, the maximum pixel value that can be attained from the JPEG format. However, I_0 must be experimentally determined to generate a continuous relationship between transmission and thickness that is accurate in the desired thickness range. Alpha also must be experimentally determined. Although it is given in literature, α is highly dependent on wavelength, and in the setup above, there is a distribution of wavelengths. Finding α experimentally adds accuracy to the thickness measurement technique.

A control wafer was designed to determine α and I_0 , calibrating the thickness imaging technique. A schematic of the control wafer is shown in Figure 34. The wafer is composed of 250 μm thick plateaus 200 μm thick valleys. Figure 34 also shows what the control wafer would look like when placed in the thickness measuring apparatus. The dark lines would represent the peaks where more light is absorbed and therefore less is transmitted, while the lighter lines

would represent the troughs. The purpose of such a control wafer is to provide two data points that we can use to experimentally solve for I_0 and α in our thickness relationship (equation 3).

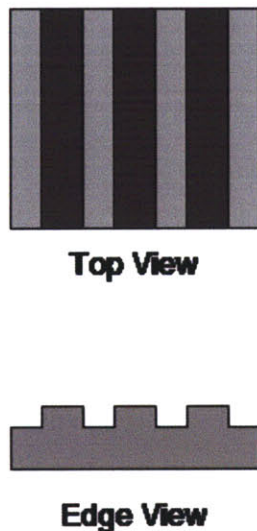


Figure 34: Schematic of the control wafer. The wafer was etched in strips to give regions of contrasting thickness and therefore contrasting brightness in thickness imaging. The plateaus are 250 μm thick and the valleys are 200 μm thick.

The average pixel value for the peaks and troughs were found, giving two distinct pairs of thickness and transmission. These pairs were substituted into equation (3) along with the reflective coefficient (dependent only on the index of refraction of air and silicon), allowing us to solve for I_0 and α , and generate a final equation relating thickness to a transmitted pixel value. The relationship is given by

$$I = 896e^{-82.5t}, \quad (4)$$

where I is pixel value and t is thickness. Shown in Figure 35 is a plot of transmission vs. thickness for a given range of thicknesses.

The absorption coefficient was found to be $\alpha = 82.5 \text{ cm}^{-1}$, compared with the standard published value of 183 cm^{-1} for 940 nm IR radiation. This lower value of α means that there is a smaller difference in the measured transmission for a given thickness difference in the wafer. This measured result is most likely due to the difference in the surface finishes of the plateaus and valleys. The surface of the plateaus was shiny and polished while the etched valleys were much rougher. This caused the measured transmission of light through the valleys to be less than it should have been, resulting in a lower value of α .

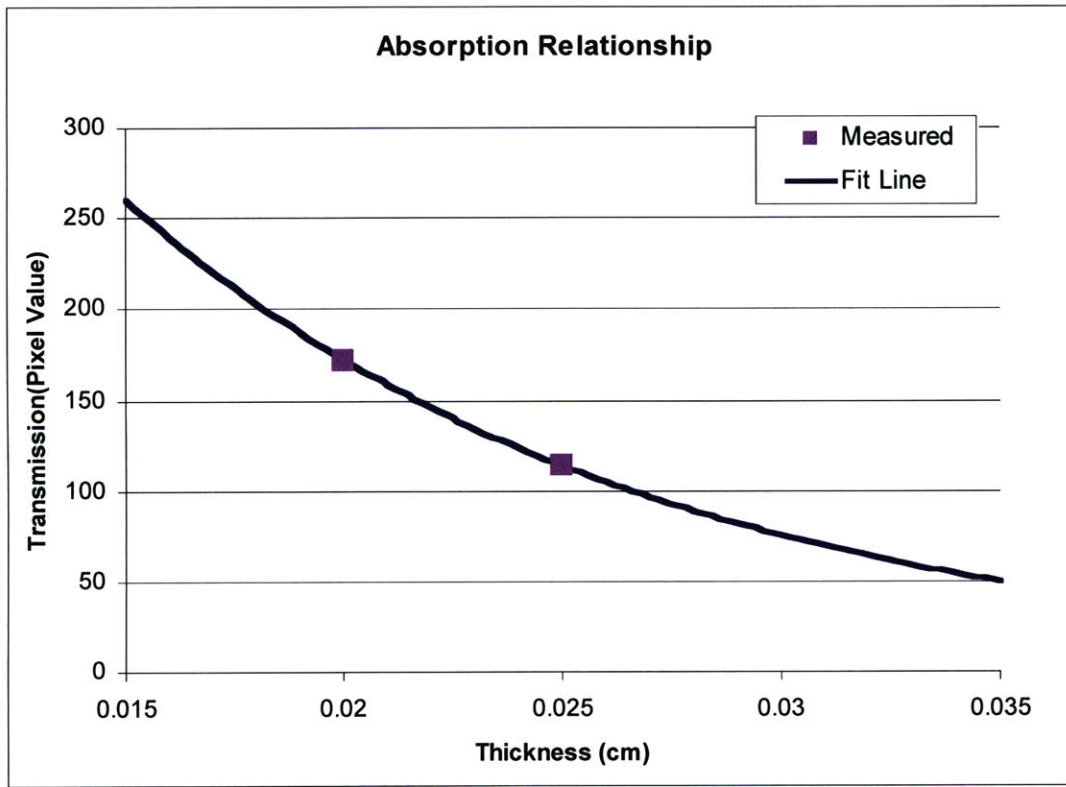


Figure 35: Graph of thickness vs. transmission for thickness between 0 and 500 μm . The graph was created with the control wafer, and will allow us to take photographs of other wafers and transform transmission data into an array of thicknesses to map a wafer's thickness.

4.4 Contour Plot Generation

After we have an equation, we are now able to generate a thickness diagram. Here, we will generate a map of the control wafer to verify equation (4) and understand how to convert to an image. The image captured by the CCD camera is shown in Figure 36. Once the image is converted to a grayscale JPEG file format, it is sent to excel as a grid of pixel values. This grid ranges in value from 0 (complete black) to 255 (complete white). To convert this data into a map, it is necessary to substitute the transmitted pixel value into equation 4 for each point in the grid. The new grid is composed of thicknesses and can be plotted in excel to give a visual picture of wafer thickness. Additionally, the data itself can be analyzed to determine the thickness range, mean thickness, standard deviation, or any other desired quantities. Shown in Figure 37 is the thickness map of the control wafer.

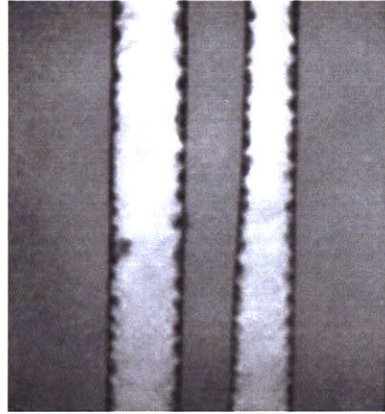


Figure 36: Image of the control wafer captured by the CCD camera in the IR thickness imaging setup. The dark areas represent the thicker, 250 μm areas, while the lighter strips represent 200 μm valleys that were etched away.

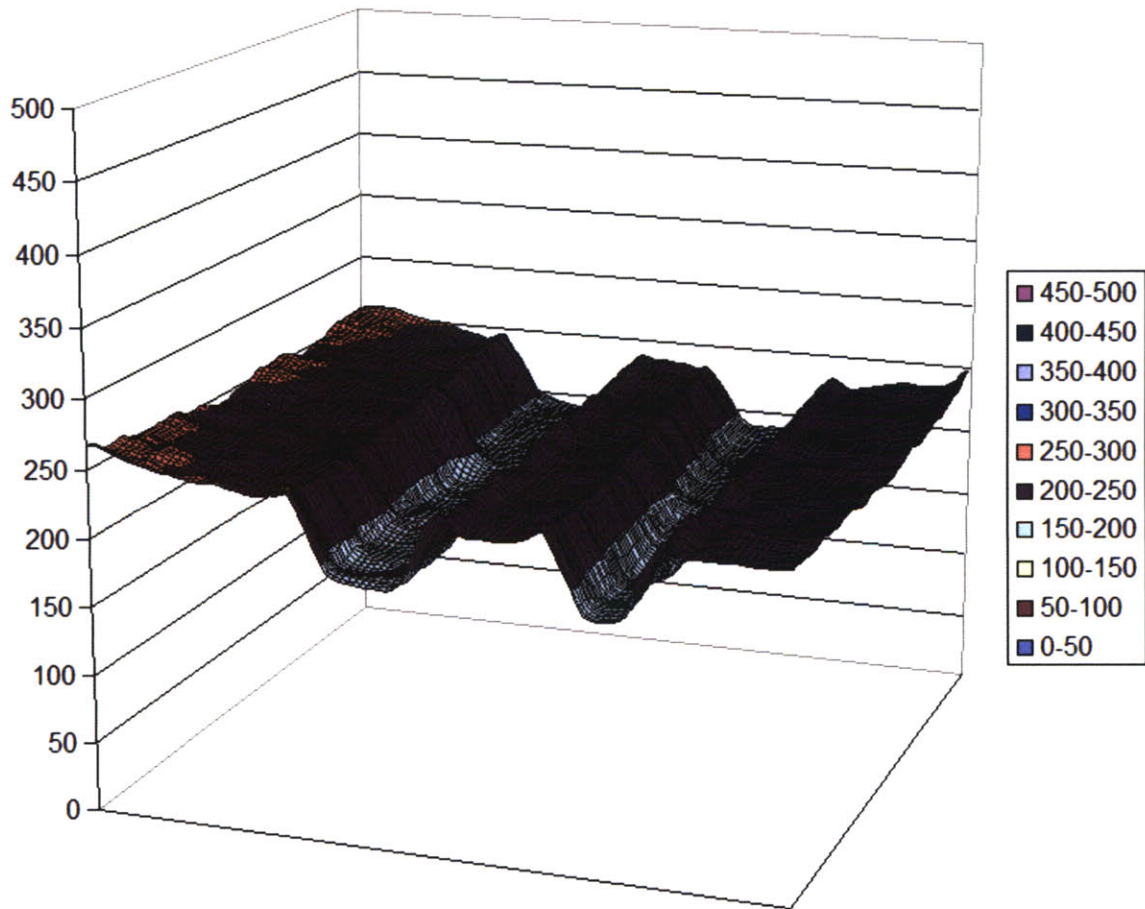


Figure 37: Contour map of the control wafer.

Chapter 5

Results and Evolution of Geometry Control

The following section shows the evolution of the geometry problem. For reference, it begins with the results obtained by having two backing plates control the geometry of the wafer. The results obtained using a powder shell to control geometry will then be examined and improvements noted. Subsequent sections reveal the evolution of the powder shell setup, and the results that go along with each modification. There are distinct reasons behind each modification in the process, and the results will display the progress that has been made.

The thickness variation as well as horizontal geometry of the recrystallized wafers were analyzed. The thickness range across a wafer as well as the value, $\frac{\sigma}{\mu}$, are used to characterize thickness variation. The standard deviation divided by the mean thickness gives a normalized measure of the variation across the wafer. It's important to note that the higher this value is, the more thickness variation exists in the wafer, and the worse the quality of the wafer.

5.1 Control: Parallel Backing Plates

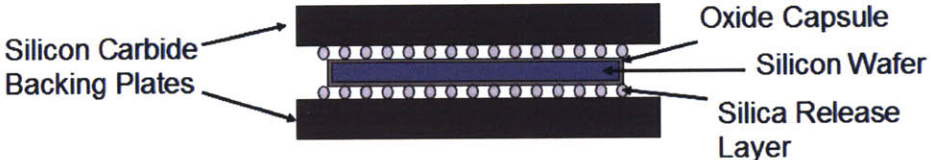
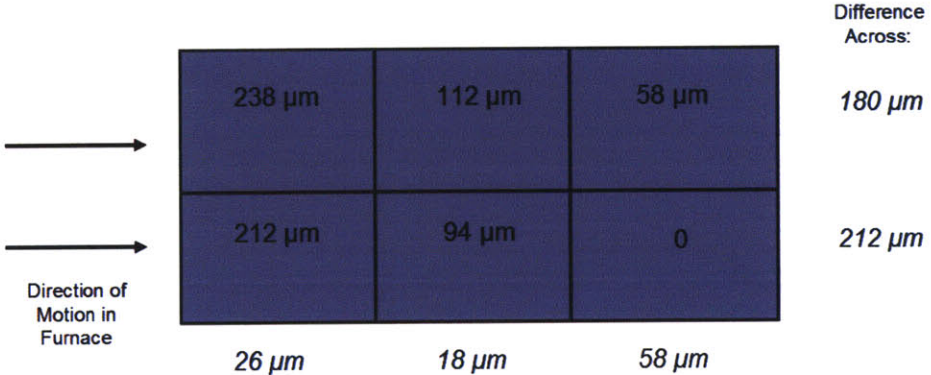
Prior to this work, parallel backing plates were used to minimize thickness variation in the recrystallized wafer. Shown in Figure 38 are the results of recrystallizing a wafer between two parallel backing plates with a release layer between the oxidized wafer and backing plates. It is first important to note the physical appearance of the wafer. The surface contains numerous indentations, and the roughness is more dramatic along the trailing edge than leading edge. From the photographs, it is also apparent that parallel backing plates do not control the horizontal geometry of the wafer. The trailing edge contains a large extrusion of silicon that clearly would need to be removed by a post processing step.

Due to the large thickness variation across the wafer, measurements were taken by hand by the procedure outlined in Chapter 4. The average thickness was found separately for six sections of the wafer, and the results are given in Figure 38. The measurements quantitatively demonstrate that the wafer recrystallized into a wedge-shaped final state. Across the length of

the wafer, there is 212 μm of thickness variation, too large to be used in actual wafer production.

The normalized variation was determined to be $\frac{\sigma}{\mu} = 0.764$, and will be compared to the other

techniques tested in this work.

<p>Schematic</p>	
<p>Thickness Diagram</p>	
<p>Normalized Variation</p>	$\frac{\sigma}{\mu} = 0.764$
<p>Top Surface</p>	

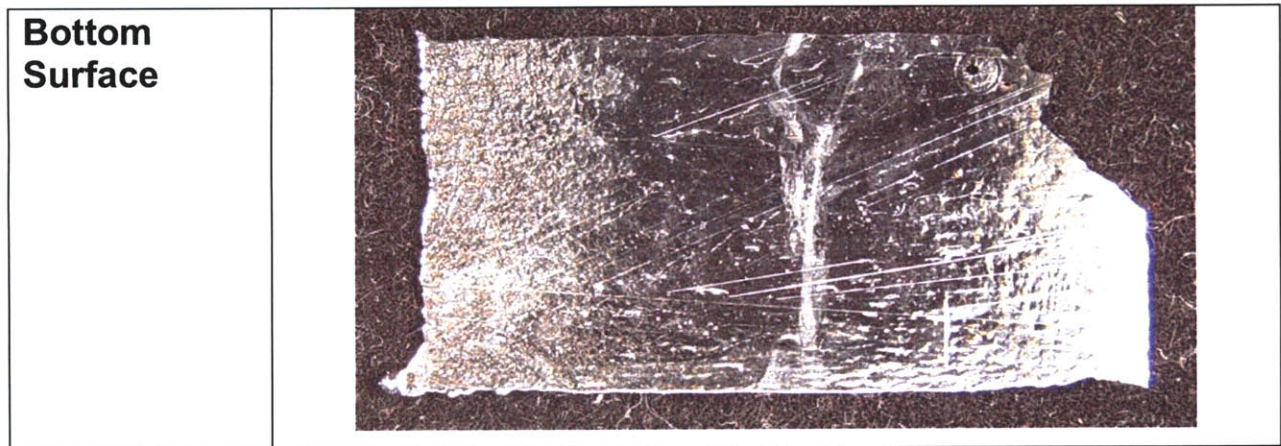


Figure 38: Results of a wafer recrystallized with parallel backing plates. The right edge of the wafer is the leading edge, and the resultant thickness difference is 212 μm across the length of the wafer. The normalized variation of $\sigma/\mu = 0.764$ is very large, indicating poor thickness control. The top photograph shows a rough surface texture (especially on the trailing edge), and the non-uniformity on the trailing edge of the wafer displays how poorly parallel backing plates preserve the geometry of a wafer during recrystallization.

5.2 Powder Shell

To improve the results of the parallel backing plate tests, a powder shell was created to encase the wafer and prevent thickness non-uniformity. Using the SiC bimodal mixture determined from extensive testing, a shell was created on top of the silicon wafer, and the entire package was sent through the recrystallization furnace. Photographs of the top and bottom surface of the recrystallized wafer are shown in Figure 39. The top surface of the wafer (the surface in contact with the powder bed) has a great physical appearance and the only imperfections are slight bumps most likely caused by non-perfect packing of the powder bed. Subsequent tests reveal that these bumps can be alleviated with thorough mixing of the powder prior to depositing it onto the wafer and backing plate. The bottom surface (the surface in contact with the release layer) however, is much more rough and exhibits increased roughness and non-uniformity on the trailing edge (The wafer entered the furnace from left to right, leaving the trailing edge on the right of the photographs of Figure 39.).

The wafer cracked during the removal of the powder shell, making us unable to capture the thickness variation using the imaging technique. Therefore, we were forced to use the initial thickness analysis technique, where the wafer was divided in six sections. A thickness diagram is shown in Figure 39, and improvement has been made over the results using parallel backing plates. The thickness variation and normalized variation have been reduced to 100 μm and

$\frac{\sigma}{\mu} = 0.264$ respectively. Although improvements have been made, thickness variation must be

reduced further to make this technique successful in production.

<p>Schematic</p>	
<p>Thickness Diagram</p>	
<p>Normalized Variation</p>	$\frac{\sigma}{\mu} = 0.264$
<p>Bottom Surface</p>	

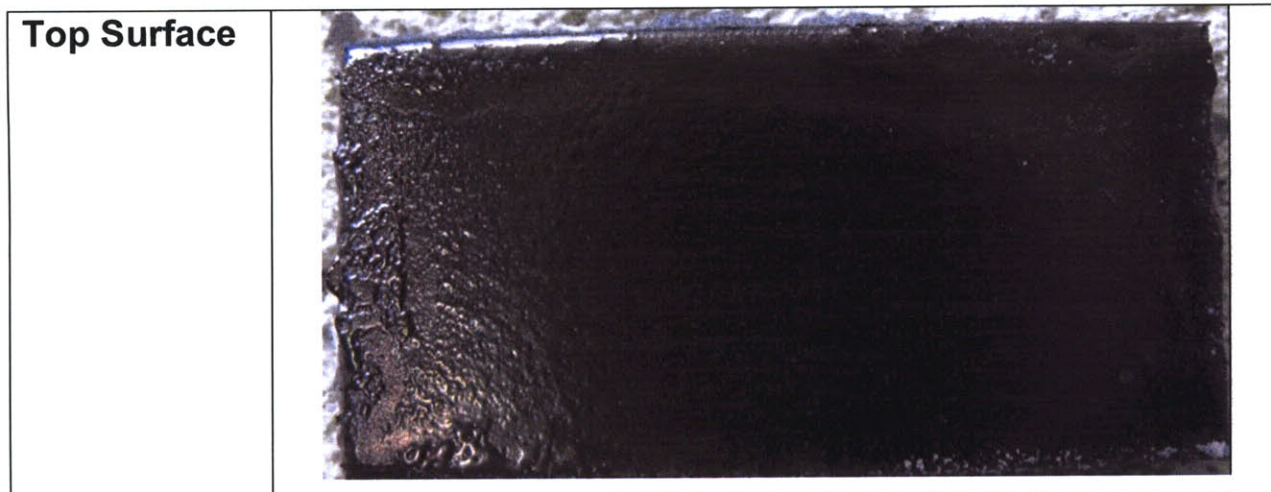


Figure 39: Results of a wafer recrystallized using the powder shell technique and a silica release layer. The right edge of the wafer is the leading edge, and the recrystallized result is an improved thickness difference of 100 μm across the length of the wafer. The normalized variation of $\sigma/\mu = 0.264$ is an improvement over parallel backing plates, indicating improved thickness control. The top surface is mostly smooth while the bottom surface has increased roughness especially on the trailing edge (left edge of photo).

Although the top surface of the wafer is generally flat with a good finish, the bottom surface contains many imperfections. The trailing edge of the wafer contains many noticeable defects and appears very rough to the naked eye. This same roughness occurs in every sample that was recrystallized with a top powder bed. The top surface of the wafer which is in direct contact with the powder bed has a great finish, but the bottom surface in contact with the release layer and backing plate has a distorted surface, which seems to contribute to the overall non-uniformity of the wafer.

5.3 Wafer Encased in Powder Shell

After observing the differences between the surfaces of a recrystallized wafer (the side that was in contact with the bed vs. the side in contact with the backing plate and release layer), we decided to attempt to embed the wafer in a powder shell so that both the top and bottom surface of the wafer are in contact with the powder bed. The same SiC bimodal powder mixture was used. The process is very similar to the initial powder shell creation method with some slight modifications. First the rubber mold is placed onto the backing plate and a thin layer of powder is poured down. The backing plate is vibrated to allow the powder to smooth and flatten, creating a platform to place the wafer on. The wafer is placed on the flattened powder layer and pressed down to ensure the powder is in contact with the entire bottom surface of the wafer. The

final steps are identical to that of the one-sided powder shell. A top powder layer is applied and compacted, the powder is sintered, and the entire package is run through the recrystallization furnace. A schematic of the setup is shown in Figure 41, and a photograph of a shell after recrystallization is shown in Figure 40. With powder on both sides of the wafer, the shell had massive cracking as it moved through the recrystallization furnace. The result was also a wafer with a great deal of thickness variation.

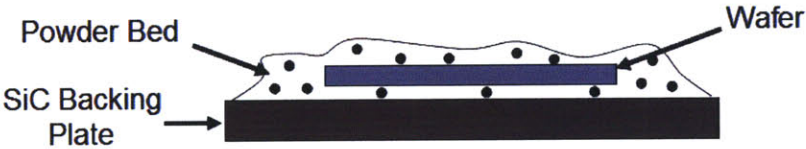
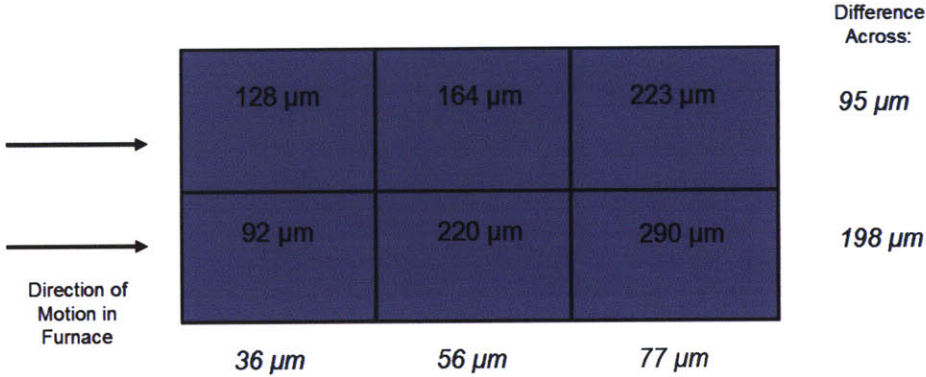
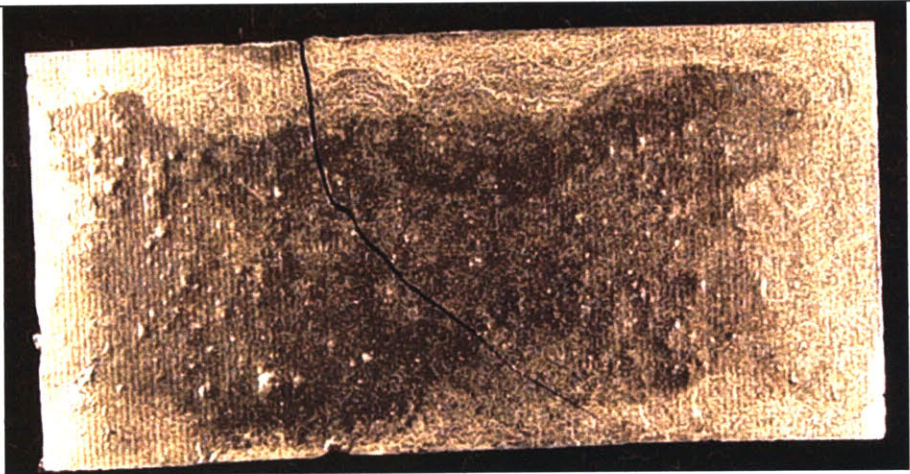


Figure 40: Photograph of powder shell following recrystallization. SiC bimodal powder completely surrounded the wafer. With powder on both sides of the wafer, the shell developed large cracks, leaving us unable to create an intact enclosure.

Photographs of the top and bottom surfaces of the wafer are shown in the bottom of Figure 41. Just as in the previous case, the top surface is very well preserved aside from a few small lumps. The bottom surface appears to contribute the majority of the non-uniformity. The pattern of a smooth leading edge and rough trailing edge is not present, but rather, the entire surface contains defects and imperfections. This is most likely the result of our inability to create a flat and uniform layer of powder in contact with the bottom surface of the wafer.

The thickness variation across the wafer recrystallized in a complete powder shell was again too large to be analyzed using thickness imaging. Measurements were taken by hand and are displayed in the thickness diagram in Figure 41. Along the length of the wafer, there was 198 μm of thickness variation, much too great to be successful in production. Although a large range, the dimensionless thickness variation was found to be below the variation of parallel

backing plates, at $\frac{\sigma}{\mu} = 0.388$. The technique is an improvement over using two backing plates, but is not as successful as the single-sided powder bed in preserving geometry.

<p>Schematic</p>													
<p>Thickness Diagram</p>	 <table border="1" style="margin-left: auto; margin-right: auto;"> <tr> <td>128 μm</td> <td>164 μm</td> <td>223 μm</td> <td rowspan="2">Difference Across: 95 μm</td> </tr> <tr> <td>92 μm</td> <td>220 μm</td> <td>290 μm</td> <td>198 μm</td> </tr> <tr> <td colspan="3" style="text-align: center;">36 μm 56 μm 77 μm</td> <td></td> </tr> </table>	128 μm	164 μm	223 μm	Difference Across: 95 μm	92 μm	220 μm	290 μm	198 μm	36 μm 56 μm 77 μm			
128 μm	164 μm	223 μm	Difference Across: 95 μm										
92 μm	220 μm	290 μm		198 μm									
36 μm 56 μm 77 μm													
<p>Normalized Variation</p>	$\frac{\sigma}{\mu} = 0.388$												
<p>Top Surface</p>													

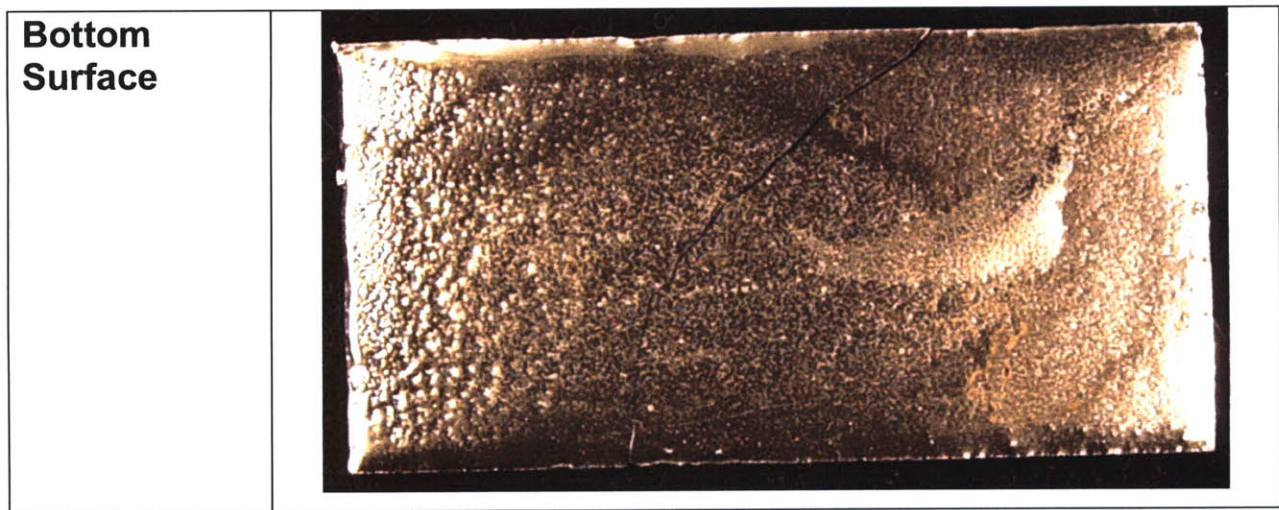


Figure 41: Results of a wafer recrystallized in a complete powder shell (powder on both sides). The right edge of the photographs is the leading edge. The resultant thickness difference is 198 μm across the length of the wafer and the normalized variation is $\sigma/\mu = 0.388$. The thickness variation is worse than the initial powder shell technique due to the inability to create an intact enclosure of powder. The top surface is relatively smooth with few sporadic bumps due to agglomeration of the powder mixture. The bottom surface contains the majority of the thickness variation due to the inability to create a flat bottom layer.

5.4 Powder Shell with Cast Release Layer

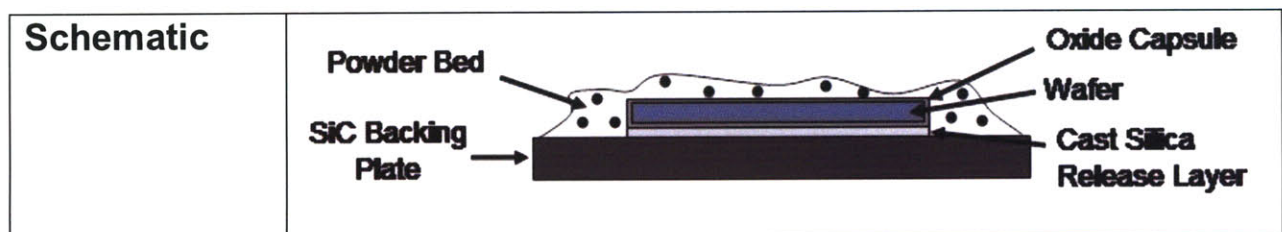
Unable to succeed in controlling geometry with a SiC powder completely encasing the wafer, we decided to revert back to the initial process of only having powder placed on top of the wafer. However, rather than applying the silica release layer by powder-coating, we attempted to create a cast silica release layer. Initially, the release layer was powder-coated onto the backing plate. Although it created an interface that would separate the backing plate from the wafer, the powder-coated layer was not very smooth, and particle agglomeration seemed to create a release layer of varying thickness. To improve this, a silica powder slurry was created by mixing silica powder and IPA. The slurry was mixed thoroughly and applied to the backing plate with a syringe. The layer was allowed to dry and the result was a dimensionally consistent release layer. A photograph of the smooth release layer following removal of a recrystallized wafer is shown in Figure 42. The layer is uniform and smooth and provides a good interface preventing the wafer from adhering to the backing plate during recrystallization.



Figure 42: Photograph of cast silica release layer after recrystallization has occurred. The wafer was easily removed from the release layer which remained flat and intact during the melting process. The layer also sintered slightly, creating a layer which would support the molten wafer.

Photographs of the top and bottom surface of the wafer are shown in the bottom of Figure 43. The appearance of the recrystallized wafer is very similar to past tests, where the top surface is intact with minor defects caused by imperfections in the top powder bed. The bottom surface is not as well preserved, but is an improvement over past tests. The surface is scalloped and rough, but the overall thickness uniformity has been greatly improved.

The recrystallized wafer cracked while trying to remove excess powder with etchant, forcing us to analyze the thickness variation with hand measurements (and not the thickness imaging technique). The thickness diagram is shown in Figure 43 displaying a drastic improvement over previous tests. The maximum thickness variation along the wafer is only 28 μm , and the dimensionless thickness variation term is also an improvement over previous attempts with a value of $\frac{\sigma}{\mu} = 0.125$.



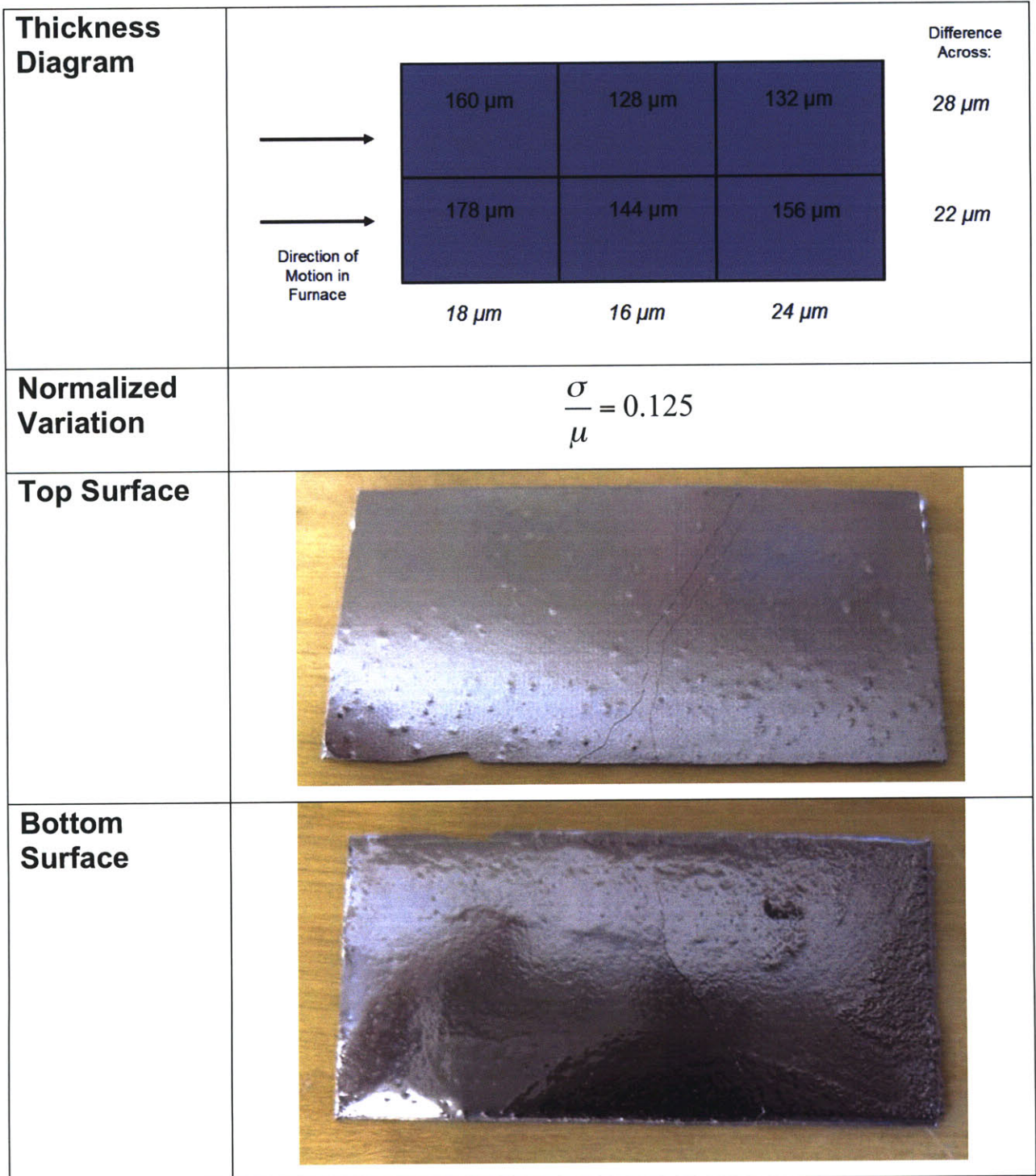
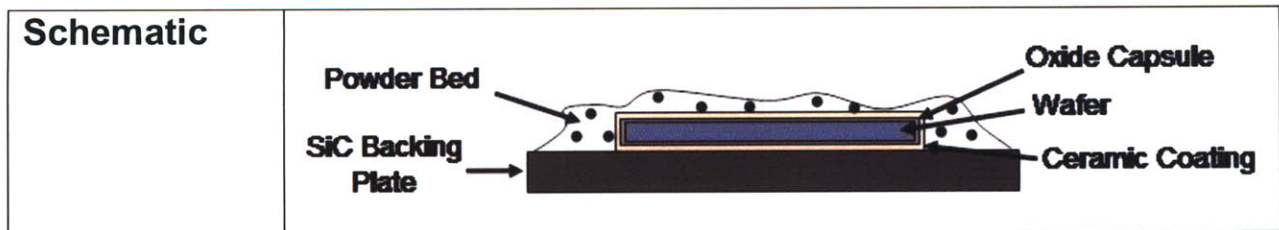


Figure 43: Results of a wafer recrystallized using the powder shell technique with a cast release layer. The right edge of the wafer is the leading edge. The technique resulted in a thickness variation of less than 30 μm across the length of the wafer; greatly reduced from other trials. The normalized variation is also extremely low at $\sigma/\mu = 0.125$. Although an improvement in thickness uniformity, the top surface has sporadic lumps due to agglomeration of powder particles in the powder shell. The bottom surface also shows a scalloped texture due to the unevenness of the cast release layer.

5.5 Ceramic Coating Technique

Photographs of a recrystallized wafer using the ceramic coating technique are shown in Figure 44. The most apparent feature of the wafer is the surface finish; far superior to wafers recrystallized with only a powder shell and no slurry coating. The top surface is nearly perfect with only slight distortion on the trailing edge (the left edge is trailing edge as wafer entered furnace from right to left). Additionally, the right edge has the text “Chris 17” still engraved in the surface. “Chris 17” was laser engraved on the wafer prior to recrystallization, and remained intact during the process, proving the extent of detail that the process is able to preserve. The bottom surface of the recrystallized wafer (the wafer entered the furnace on the right, with the trailing edge being the left edge of the picture) also contains an excellent surface finish that is consistent with the top of the wafer, and grain structure is also visible. However, all four edges of the bottom surface are slightly raised from the bulk of the wafer. This distortion is most likely a result spin coating the ceramic slurry onto the wafer. The edges of the coating were distorted, resulting in a distortion of the final, recrystallized wafer.

The thickness diagram of the recrystallized wafer is shown in Figure 44 displaying relatively good thickness variation. The maximum thickness variation along the wafer is $64\ \mu\text{m}$, while the dimensionless thickness variation has a value of $\frac{\sigma}{\mu} = 0.128$. Although the variation is not as minimal as with the cast release layer, the ceramic coating technique is an improvement over parallel backing plates and the powder shell technique. Additionally, the ceramic coating results in a recrystallized wafer with an extraordinary surface finish.



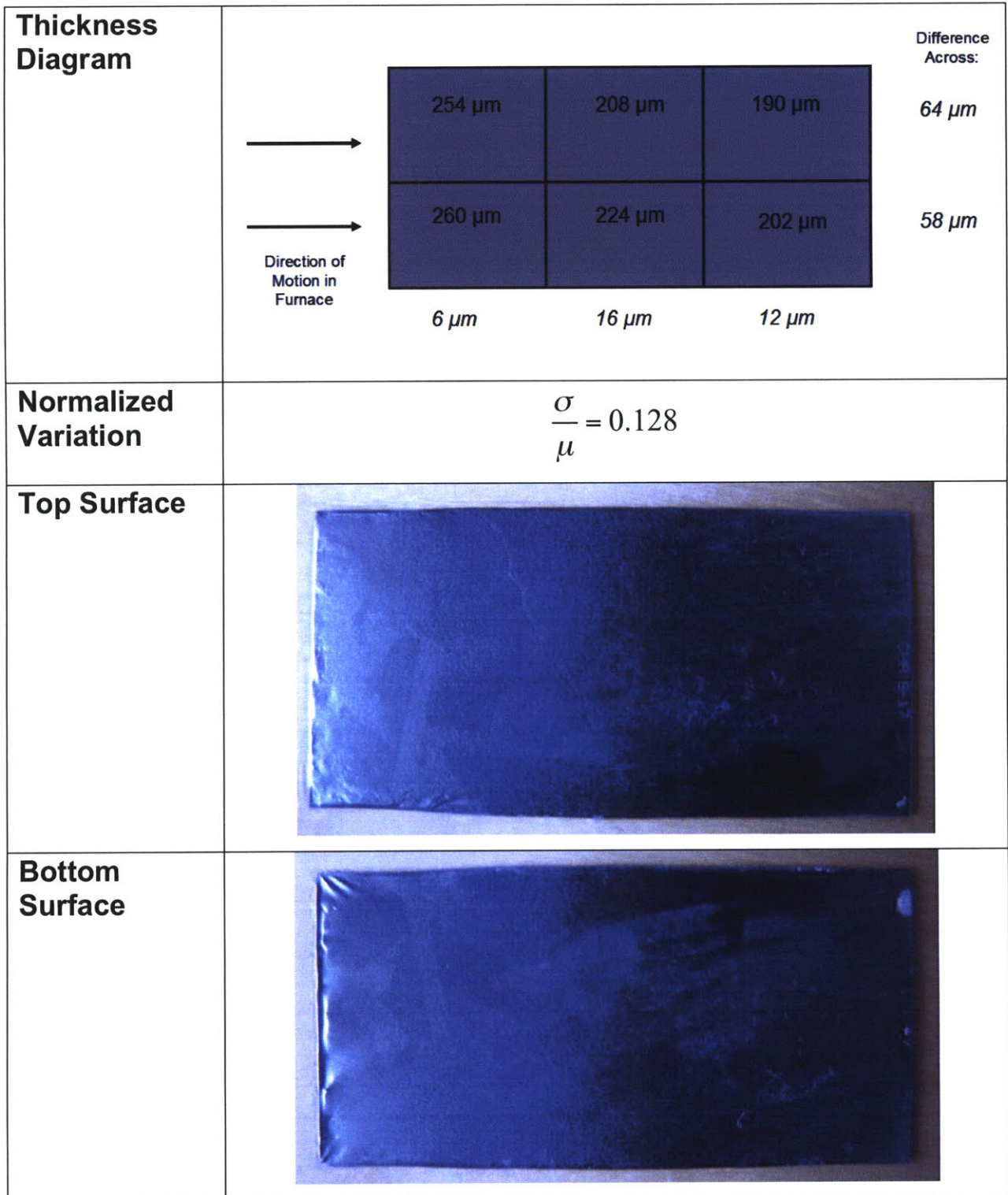


Figure 44: Results of a wafer recrystallized using the ceramic coating technique. The right edge of the wafer is the leading edge, and the technique resulted in a thickness variation of 64 μm across the length of the wafer. The normalized variation is also extremely low at $\sigma/\mu = 0.128$. Although slightly worse than the cast release layer method, the ceramic coating method shows a drastic improvement in surface finish on both the top and bottom surfaces of the recrystallized wafer.

5.6 Additional Tests Using Ceramic Coating Technique

Additional possible benefits of recrystallization using the lost-foam casting technique were tested and the results are given in this section. From Section 6.5, we accidentally discovered that the lost-foam casting technique had the ability to preserve the laser engraving initially present on the wafer. Following this discovery, we explored further how well the process could preserve details on the wafer. Additionally, because of the excellent shell created by the ceramic slurry, it may not be necessary to grow the initial oxide capsule on the wafer. The 20 hour oxidation at 1100 C is an important step in the process, and a step that has a potential of ruining the electrical efficiency of the resultant wafer. When the wafer is exposed to high temperatures for a long duration, impurities have the ability to diffuse into the wafer, disrupting its electrical properties. The following is a description of these investigations.

5.6.1 Detail Preservation

An additional technology has been developed by Ely Sachs to improve the efficiency of solar cells created with multi-crystalline Silicon wafers. The general idea is to improve the light trapping ability of cells by creating grooves on the surface of the wafer. These grooves refract incoming light at various angles, increasing the distance light travels in the wafer, and therefore, increasing the total amount of light that gets absorbed and converted to electricity. The grooves are semi-circular indentations in the surface of the wafer and are approximately 20 μm and 20 μm deep. Shown in Figure 45, is a SEM micrograph of a textured surface after it has been recrystallized using the lost foam casting technique. The micrograph shows that the texture was preserved very well, with few if any imperfections in the texture.

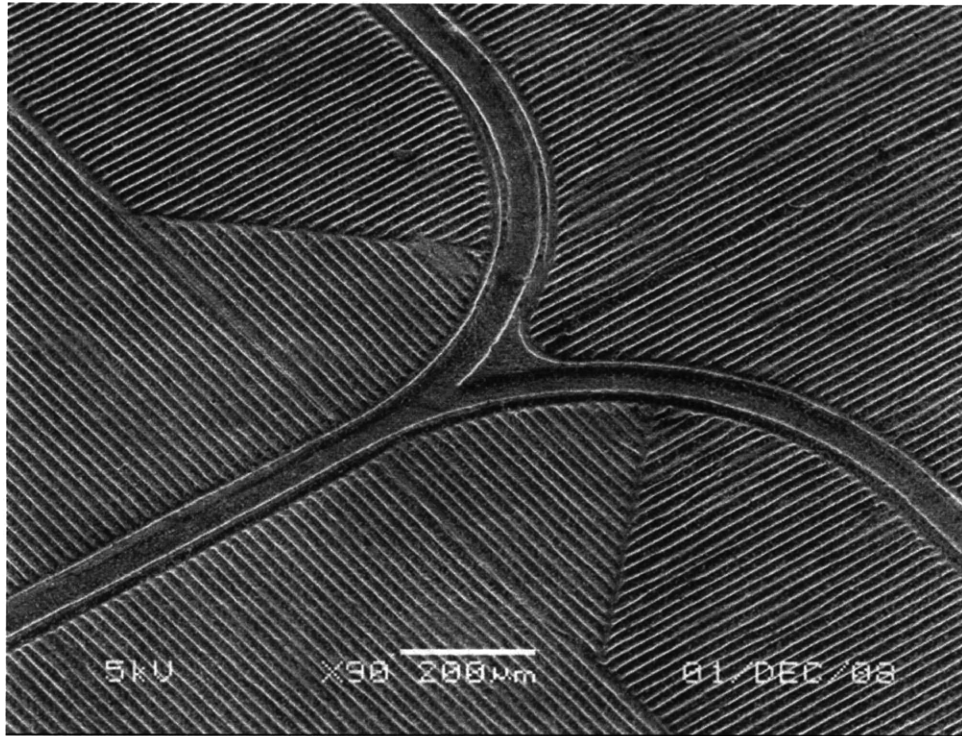


Figure 45: SEM Micrograph of a textured wafer that was recrystallized using the lost-foam casting technique. The texture is 20 μm wide trenches that are used to increase the light trapping ability of the wafer in solar applications. The texture was preserved quite well with the SiC coating, suggesting that it would be possible to create the texture prior to recrystallization.

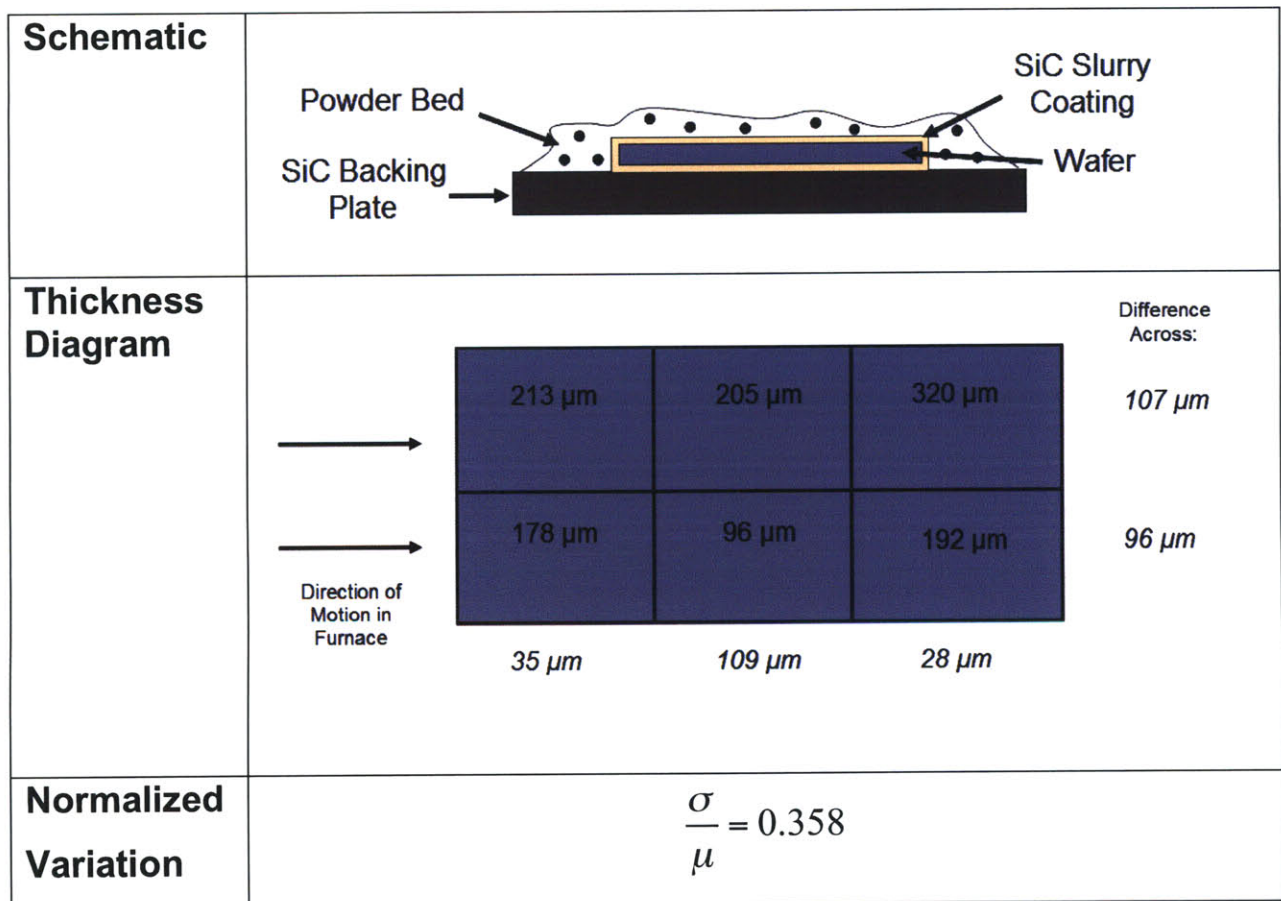
The results of this trial suggest that the entire geometry of the wafer can be created prior to the recrystallization step. Not only can the size and shape of the wafer be determined, but the surface texture can also be created, resulting in zero geometry alterations following recrystallization.

5.6.2 Recrystallization with Thinner Oxide Capsule

In addition to preserving fine detail, we also wanted to determine how well the slurry coating would encase the wafer. In all prior tests, before entering the recrystallization furnace, an oxide capsule was grown around the test wafer to contain the molten silicon and prevent it from leaking out into the powder shell surrounding the wafer. The 1 μm thick oxide is created by heating the wafer to 1100 C for 20 hours. This long oxidation period allows impurities in the oxidation furnace to diffuse into the wafer, reducing the electrical properties of the final wafer. If the length of this step in the manufacturing process could be reduced (indicating that a thinner oxide was sufficient), the electrical performance of the final solar cell could be greatly improved. In fact, no prior oxidation period may be necessary, as oxidation occurs during the

recrystallization step itself. As the wafer moves through the furnace and is heated, a thin oxide grows on the wafer surface.

Shown in Figure 46 are the results of recrystallization using the ceramic coating method in which no oxide was grown on the wafer prior to entrance in the recrystallization furnace. The only oxide present on the wafer arose as the wafer moved through the recrystallization furnace. The recrystallization was successful, producing a wafer with a surface finish on par if not superior to the trial with an oxidized wafer. The top surface is near perfect with a great finish, and the bottom surface is also impressive, with slight bumps present on the trailing edge. The thickness variation is worse than the case of an oxidized wafer but more importantly, this trial shows successful recrystallization with a thin oxide capsule, created only as the wafer passed through the recrystallization furnace (and not in a prior step).



<p>Top Surface</p>	
<p>Bottom Surface</p>	

Figure 46: Results of a wafer recrystallized using the ceramic coating technique with no oxide capsule. The right edge of the wafer is the leading edge, and the technique resulted in a thickness variation of 107 μm across the length of the wafer. The normalized variation is also extremely low at $\sigma/\mu = 0.358$. Although worse than the case where an oxide capsule was used, the test displays that the oxide capsule is not needed with the ceramic coating technique.

Chapter 6

Conclusions

The goal of the research was to improve the thickness variation of wafers during the recrystallization process. Initially, parallel backing plates were placed above and below a wafer in hopes of maintaining the wafer's initial geometry. Other methods were tested, and the results are given in Table 1. Two important measures were used to determine how uniform a wafer was upon exiting the recrystallization furnace: the thickness range and $\frac{\sigma}{\mu}$, the standard deviation of thickness divided by the mean thickness. Each new method tested was an improvement over the initial technique using parallel backing plates. The technique using a top powder bed and cast release layer provided the best thickness control during recrystallization.

Method	Thickness Range (μm)	Normalized Variation ($\frac{\sigma}{\mu}$)
Parallel Backing Plates	212	0.764
Powder Shell	100	0.264
Powder Shell: on top and bottom of wafer	198	0.388
Powder Shell: with cast release layer	28	0.125
Ceramic Coating: oxide capsule	64	0.128
Ceramic Coating: no oxide capsule	107	0.358

Table 1: The results of each technique for preserving wafer geometry during recrystallization. The range of thickness and the normalized variation is given for each trial. The technique using a powder shell with a cast silica release layer did the best job of preserving geometry.

Although a powder shell with a cast release layer is quantitatively the best candidate for use in production, the ceramic coating technique is the preferred method. Not only does the ceramic coating technique produce a wafer with excellent surface finish, but it also has added benefits. One added benefit is the ability to preserve detail. This allows wafers to be textured prior to recrystallization, so that all geometry can be determined before the electrical properties of the wafer are improved. Additionally, the ceramic coating technique has been shown to be successful in recrystallizing a wafer with only a thin oxide capsule grown as the wafer moved through the recrystallization furnace. The need for only a thin oxide capsule could eliminate the need for a long pre-oxidation growth period that adds extra contaminants to the final wafer.

References

- [1] “Oil Demand”, Weekly Indicators - The Economist, Nov. 18, 2008, Online article, (http://www.economist.com/markets/indicators/displaystory.cfm?story_id=12607120&fsrc=rss).
- [2] Schaefer, Mike, “The Truth about Oil, Part 2”, Online article, 12 January, 2007, <http://www.energyandcapital.com/articles/oil-reserves-decline/340>.
- [3] “Fossil Fuel”, Online article, http://en.wikipedia.org/wiki/Fossil_fuel.
- [4] “Global Warming”, Online article, http://en.wikipedia.org/wiki/Global_warming.
- [5] “Renewable Energy”, Online article, http://en.wikipedia.org/wiki/Renewable_energy.
- [6] Hantsoo, Eerik T., “Silicon Cast Wafer Recrystallization for Photovoltaic Applications”, Masters Thesis, MIT, June, 2008.
- [7] German, Randall. Powder Metallurgy Science. Second Edition, Princeton, NJ: Metal Powder Industries Federation, 1994.
- [8] Suslick, Kenneth S., “The Chemical and Physical Effects of Ultrasound”, Online article, <http://www.scs.uiuc.edu/suslick/execsummsono.html>.
- [9] Lame, O., et al. “In situ Microtomography Study of Metallic Powder Sintering”, Online publication, <http://www.esrf.eu/UsersAndScience/Publications/Highlights/2002/Materials/MAT3>.
- [10] Kopeliovich, Dmitri, “Die Pressing of Metallic Powders”, Online article, http://www.substech.com/dokuwiki/doku.php?id=die_pressing_of_metallic_powders.
- [11] Gregorski, Steven J., “High Green Density Metal Parts by Vibrational Compaction of Dry Powder in the Three Dimensional Printing Process”, PhD Thesis, MIT, June, 1996.

Appendix A: Powder Selection

After developing the process plan to create a shell of powder to encapsulate the wafer during recrystallization, it was first necessary to choose an appropriate powder/powder mixture. Although there are rules and guidelines for creating a solid structure by maximizing powder sintering, in the end, the optimal powder must be experimental determined. Following the extensive theory researched in the preceding work, we tested a multitude of powders to determine which one would provide an optimal powder shell to retain the wafer during recrystallization.

Powders were tested to determine how well they would create a powder shell rather than testing how well they would actually retain the wafers due to the frailty of the recrystallization furnace. The wafers were qualitatively examined to see how well they held their shape and how rigid of a structure they created to retain the wafer.

The foremost requirement of a powder is that it does not present impurities or certain metals to the molten wafer. Therefore it must be solely comprised of silicon compounds such as silicon oxide (also known as silica with the chemical formula, SiO_2) and silicon carbide (SiC). These two compounds were the main powders tested to be implemented in the powder shell. Other powders were also tested, such as spherical alumina, so that we could test how spherical powders would sinter into a powder shell. Various powder compositions and mixtures were tested beginning with simple, single constituent powders, and moving to more complex powder mixtures.

Testing Setup and Procedure

The powder to be tested was first chosen and powder mixtures were thoroughly mixed to ensure homogeneity. A SiC backing plate is cleaned and lightly coated with fine Silica powder to provide a release layer for the wafer. The powder is powder-coated on the surface, to provide a light, even coat of powder to the surface. With the release layer in place, a silicon wafer (20mm x 40mm and 180 μm thick) is placed onto of the silica powder with care to ensure not to disturb the powder layer.

With the wafer in place, a bed of powder is then poured onto of the wafer and backing plate. For the test, powders were all slurry cast on the wafer to provide a dense, compact bed of

powder. To cast a powder layer, the powders were first mixed with IPA, resulting in a viscous slurry that could be easily applied. Shown in Figure A1 is a photograph of applying the powder bed with a slurry. A rubber mold is glued on the top of the backing plate, leaving space around the wafer and creating a seal for the slurry to be poured on top. The slurry is poured into the mold, to the height of the mold, approximately one centimeter thick, and allowed to dry in air for approximately one hour. The rubber mold is carefully removed from the backing plate without disturbing the dry, compact powder layer.

The powder bed is then sintered, to create a rigid shell from the loosely placed powder. To accomplish this, the entire apparatus (backing plate, release layer, wafer and powder bed) is heated to 1200 C for one hour. The wafer is placed into and removed from a slightly cooler environment to prevent an excess of thermal stress from cracking the powder bed and backing plate. The sintering conditions of 1200 C for one hour was chosen as an upper bound for the amount of time a wafer would be allowed to be at high temperatures. As mentioned throughout this report, when silicon is raised to high temperatures (even temperatures below its melting point), impurities are able to enter the wafer resulting in a less-efficient solar cell. Therefore, sintering time must be minimized, and one hour at 1200 C was chosen as an acceptable duration and temperature.



Figure A1: Photograph of powder slurry cast on top of the wafer and backing plate. The orange frame is a 1 cm thick piece of silicone rubber used as a mold to contain the slurry as it is poured over the wafer and backing plate. The grayish middle rectangle is the powder slurry after it has been allowed to set in air. The rubber mold is subsequently removed and the powder is sintered in a box furnace.

After sintering, the entire setup was removed from the furnace and allowed to cool in air. The cooled apparatus was then examined qualitatively to determine how well it sintered and how

well it created a case that would contain the wafer in a subsequent recrystallization step. The two main things examined were the rigidity of the shell, and the shape preservation. Shape preservation asks the question, was a good capsule created, or did the shell crack which would not retain molten silicon. The following tests examine a wide range of powder and how well they would retain a wafer during recrystallization.

There are two photographs of each powder tested. The first photograph shows the shell directly after being removed from the furnace. After cooling, the powder shell was then disturbed to determine how well it sintered into a monolithic shell. The shell was poked and pried with a tweezers, testing its rigidity and durability.

Single Constituent Powders

Silica Powder

Two different particle size silica powders were tested; 20 um and 44 um. Photographs of a powder shell created with 20 um silica powder is shown in Figure A2. The silica powder did not create a good shell to encase the wafer. Directly upon exiting the sintering furnace, the shell is weak and brittle. The top layer of powder was mildly sintered in a thin layer, but the inner powder remained soft and feathery, with essentially no sintering occurring. Overall, 20 um silica powder is not a good candidate for creating a rigid shell to encase the wafer.

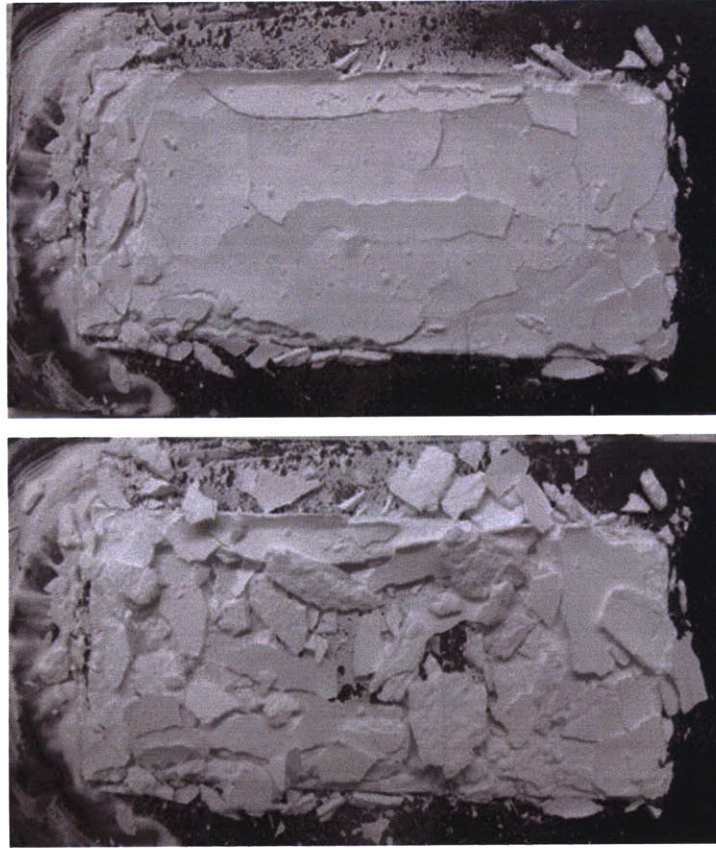


Figure A2: Photographs of a sintered powder shell created with 20 μ m silica powder. The top photograph was taken directly after the backing plate was removed from the sintering furnace while the bottom photo was taken after the powder was disturbed. The shell cracked during sintering resulting in a very brittle and weak structure that is not a good candidate for geometry control during recrystallization.

A shell created with coarser silica powder (44 μ m) was then tested and is shown in Figure A3. Although a slightly better shell was created, the coarser powder did have some of the same downfalls as the 20 μ m powder. Directly after removal from the furnace, the shell appears to have been sintered effectively. Despite a crack through the center of the shell, it appears to be very uniform and intact (as opposed to the cracked shell created with 20 μ m powder). However upon disturbing the powder bed, we are able to reveal that the powder did not, in fact, sinter well. As with the 20 μ m silica, a top thin layer of powder sintered, while inner powder did not fuse. Additionally, as can be seen clearly in the second photograph of figure 10, the powder sintered in sections, but not into a single, rigid shell. Overall, 40 μ m silica powder did not create a shell capable of retaining a silicon wafer during recrystallization.

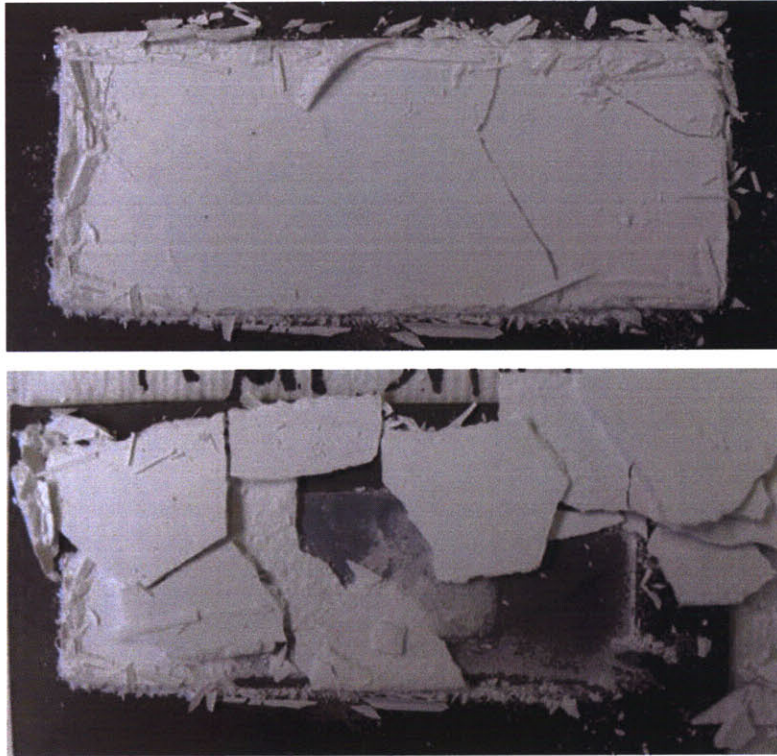


Figure A3: Photographs of a sintered powder shell created with 40 μm silica powder.

Silicon Carbide (SiC) Powder

Multiple size silicon carbide powders were then tested using the same procedure as before. Fifteen micron (15 μm) powder was first tested and is shown in figure 11. The 15 μm SiC powder sintered much better than both silica powders, but still did not result in a completely rigid shell. Although a relatively smooth shell was created, a large crack developed through the center of the shell as apparent in the first photograph of Figure A4. The shell did not withstand being disturbed and a chunk of the shell directly on top of the wafer easily broke away. The enormous crack through the center of the shell was most likely a result of shrinkage during sintering, driving a shift to a larger powder size.

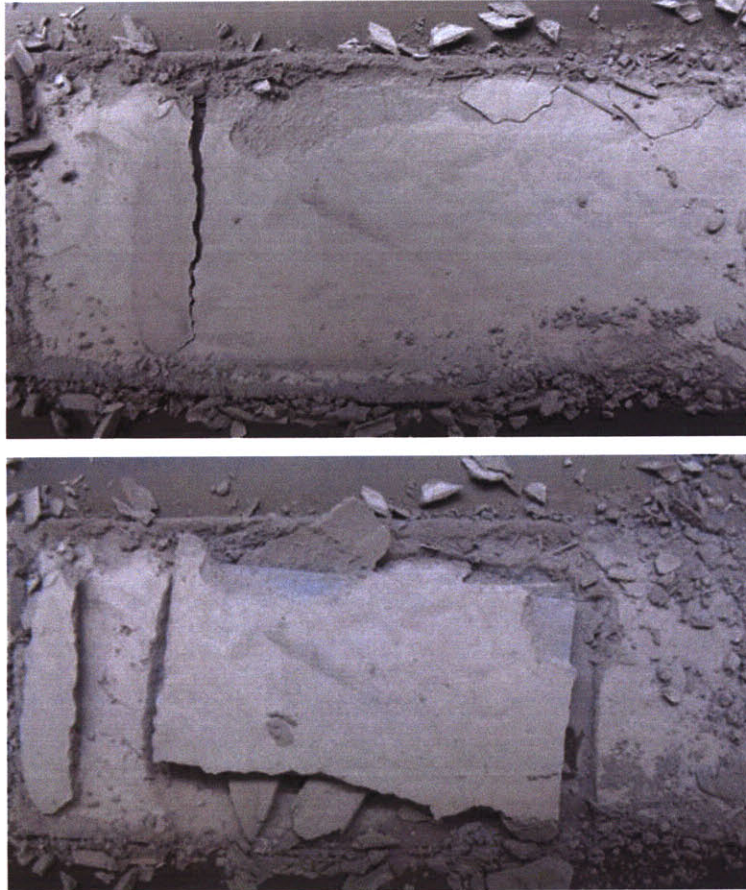


Figure A4: Photographs of a sintered powder shell created with 15 μm SiC powder.

Larger particle size SiC powder (44 μm) was then tested and is shown in Figure A5. The top photograph shows absolutely no cracking taking place in the shell during sintering. The contour lines that are visible on the top surface of the shell are a result of the slurry drying and have not impact on the structure of the shell itself. Although no cracks formed, the resultant shell was not very rigid. Again, the wafer could be removed from the powder bed easily, showing that the larger particle size did not sufficiently sinter.

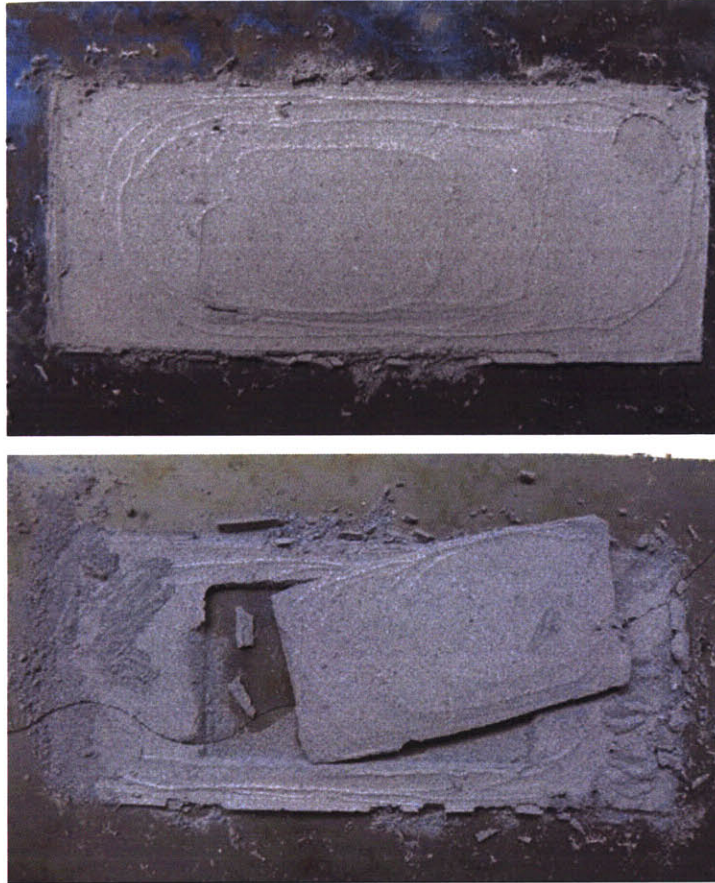


Figure A5: Photographs of a sintered powder shell created with 44 μm SiC powder.

Spherical Alumina Powder (Alumabeads)

Spherical alumina powder was the final single-constituent powder tested. The purpose of this test was to determine how well spherical particles would sinter vs. traditional powders which are much more rough. Alumina itself would not be a good material to use during recrystallization as it contains aluminum, a substance that destroys cell efficiency if it diffuses into the wafer. Two different alumabeads were tested to determine how well spherical powders would create a shell to retain the geometry of a silicon wafer during recrystallization; 10 μm and 30 μm particle size powders.

Photographs of a shell created with 10 μm Alumabeads is shown in Figure A6. The shell did not crack at all due to the extraordinary ability of spherical particles to pack efficiency when poured. The dense powder bed initially set, did not allow for shrinkage to occur and therefore, eliminated cracking that was evident in traditional powders. However, a rigid shell was not created with the spherical powder. The powder sintered somewhat, but the result were “cakes,”

or multiple individual sintered areas that were apparent after disturbing the bed (shown in the second photograph of figure 11). The shell did retain an indent of the wafer itself, as also can be seen in the second photograph of figure 11. This is a result of excellent packing achieved by the spherical particles. However, the shell was not rigid nor durable enough to be a good candidate to encase the wafer during recrystallization.

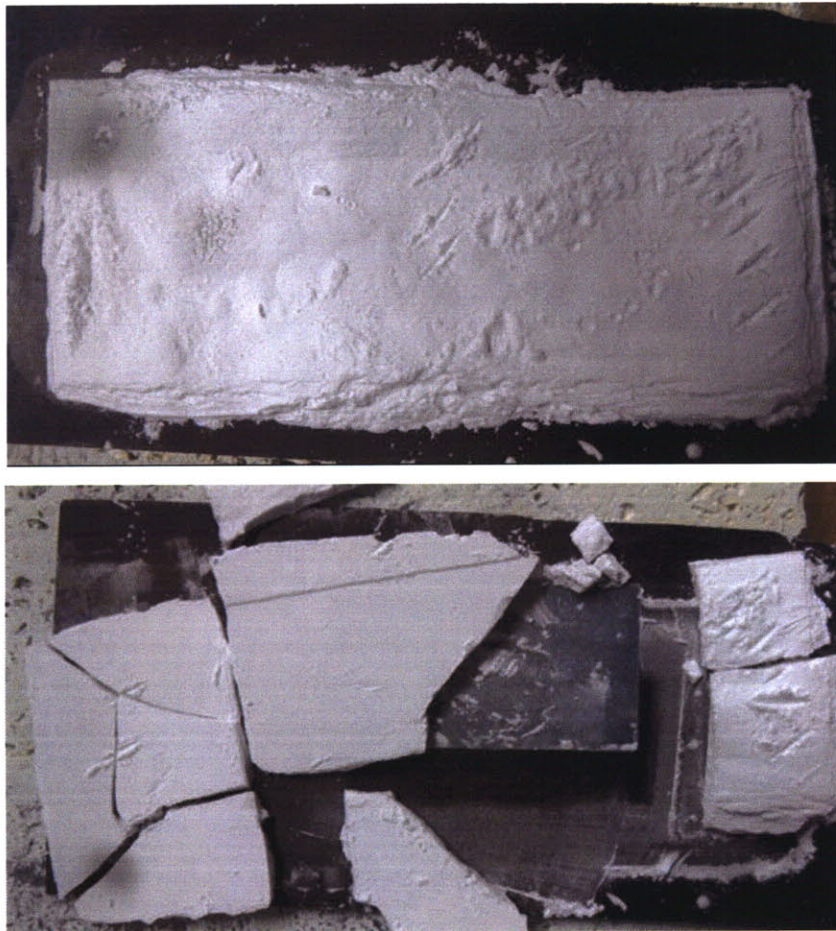


Figure A6: Photographs of a sintered powder shell created with 10 μm spherical alumina powder (Alumabeads).

A shell composed of 30 μm Alumabeads is shown in Figure A7. Different from the other powders tested, moving to a larger alumina powder actually resulted in a poorer shell. Again, the shell did not crack during sintering, and cakes were formed within the powder bed. The cakes crumbled easier than in the 10 μm Alumabeads, and overall a rigid shell was not created. However, the shell did also have a sharp indent of the wafer in it, displaying good packing occurred.

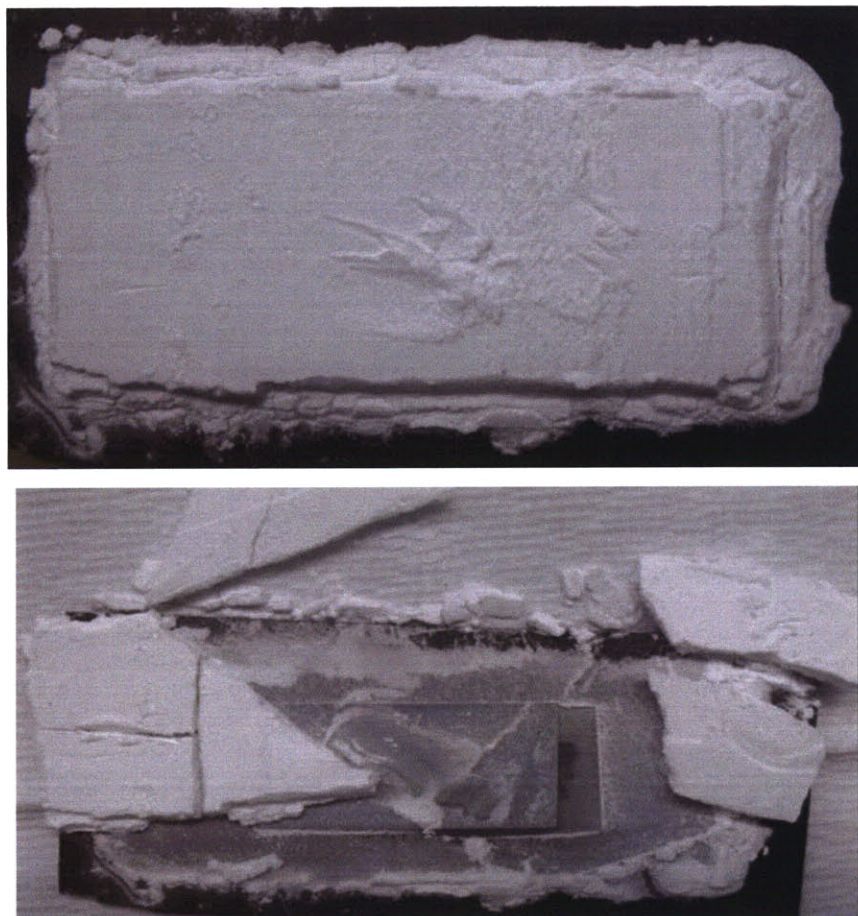


Figure A7: Photographs of a sintered powder shell created with 30 μm spherical alumina powder (Alumabeads).

Bimodal Powders

With single constituent powders unable to create a good shell to retain the wafer during recrystallization, we then moved to powder mixtures in hopes of creating a more rigid, monolithic shell.

Silica Bimodal Mixture

A photograph of a powder shell created with a silica bimodal mixture is shown in Figure A8. The mixture was created with submicron and 40 μm silica powders in a 3:1 ratio. The mixture created a shell that was an improvement over the initial silica powders but still not strong enough to succeed in recrystallization. The powder developed a thin, rigid outer layer, with a very fluffy and non-rigid interior. The shell also developed a multitude of cracks and did not pack well in contact with the wafer itself. Overall, the bimodal mixture was not a good candidate for encasing the wafer during recrystallization.

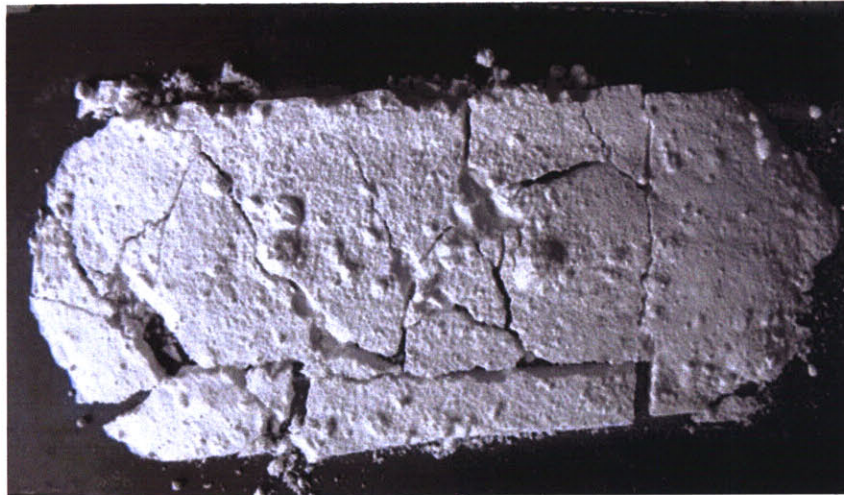


Figure A8: Photographs of a sintered powder shell created with bimodal silica composed of 40 μm silica and fines (sub micron silica powder).

SiC/Silica Bimodal Mixture

Two bimodal mixtures of silicon carbide and silica powders were tested on their ability to create a rigid shell encasing a silicon wafer. A shell created with a mixture of 45 μm silica and 2.5 μm SiC powders is shown in Figure A9. The shell didn't sinter well but rather formed a pudgy-like compound after firing. Although the powder did not join to create a rigid shell, weak bonds were formed between particles, almost as if glue had been added to the mixture. Overall, the powder joined somewhat and formed a nicely shaped shell over the wafer. However, the rigidity of the structure was insufficient to provide good support during recrystallization.

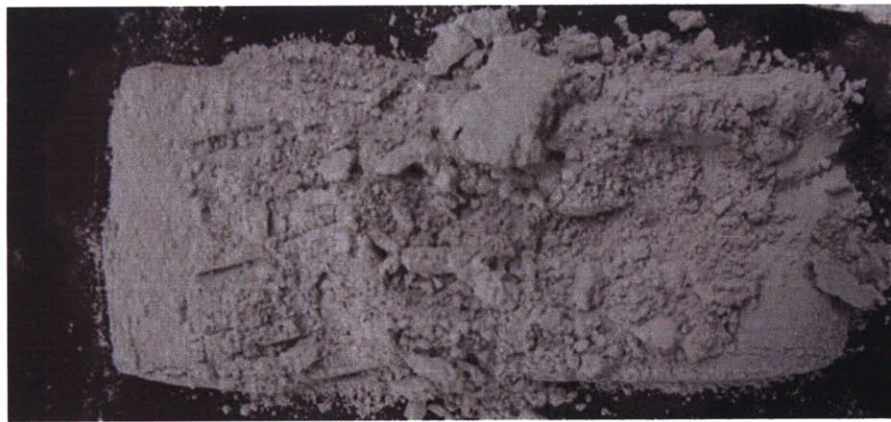
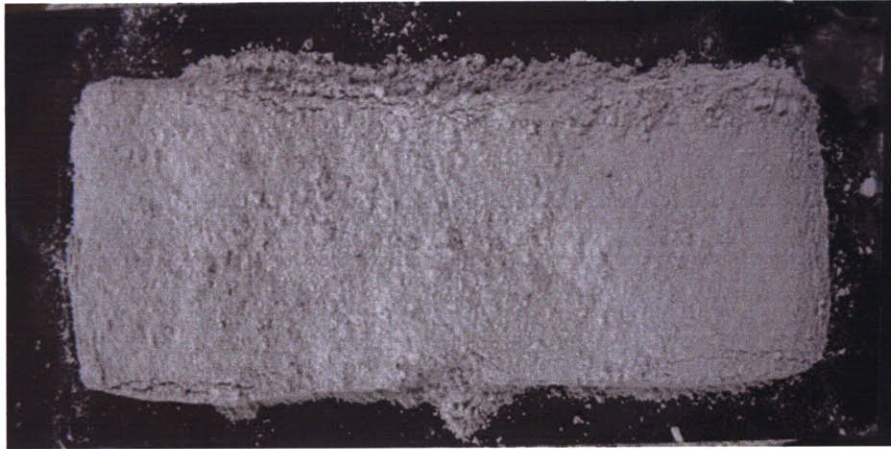


Figure A9: Photographs of a sintered powder shell created with silica/SiC bimodal mixture composed of 45 μm silica and 2.5 SiC powder.

A shell was then created with coarse silicon carbide powder and silica fines. Photographs of a shell created with 44 μm SiC powder and silica fines are shown in Figure A10. The shell maintained its shape around the wafer without any cracking or deformation. However, as apparent in the second photograph of Figure 20, the shell broke apart easily after being disturbed. The powder sintered only slightly, resulting in a shell that broke into smaller fragments relatively easily. It is also important to note that the two powders did not mix well. The large bumps in the photographs are actually particle agglomerations. These agglomerations result in less fine powder available to fit interstitially between large particles, negating the advantage of using a bimodal mixture. Overall, the SiC/silica mixture did not create a shell rigid enough to preserve a wafer during recrystallization.

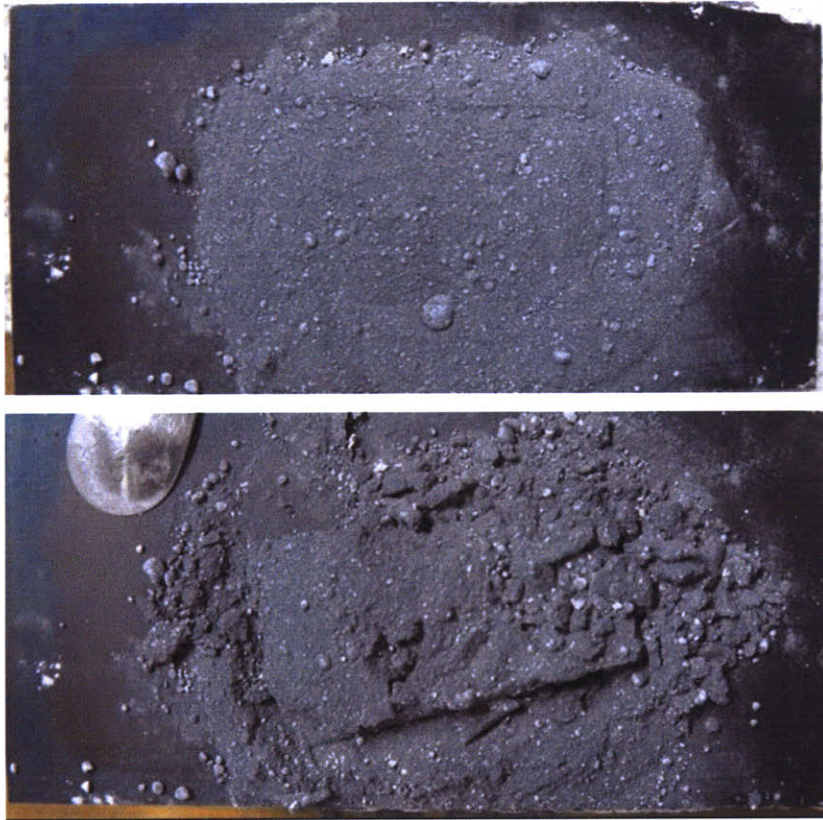


Figure A10: Photographs of a sintered powder shell created with silica/SiC bimodal mixture composed of 44 μm SiC powder and silica fines.

SiC/Alumina Bimodal Mixture

A bimodal mixture with SiC and spherical alumina powders was tested on its ability to create a shell that could retain a wafer during recrystallization. The mixture composed of 30 μm spherical alumina and 2.5 μm SiC powders is shown in photographs in Figure A11. The powder bed withstood the sintering furnace without cracking or deforming. The resultant shell displayed an excellent mold of the wafer, as can be seen in the second photograph of Figure A11. Although not an indestructible shell, the powder sintered well enough to create a semi-rigid shell that formed an excellent case around the wafer. Overall, the shape preservation and semi-rigidity of the shell make this powder mixture a good candidate for containing a wafer during recrystallization.

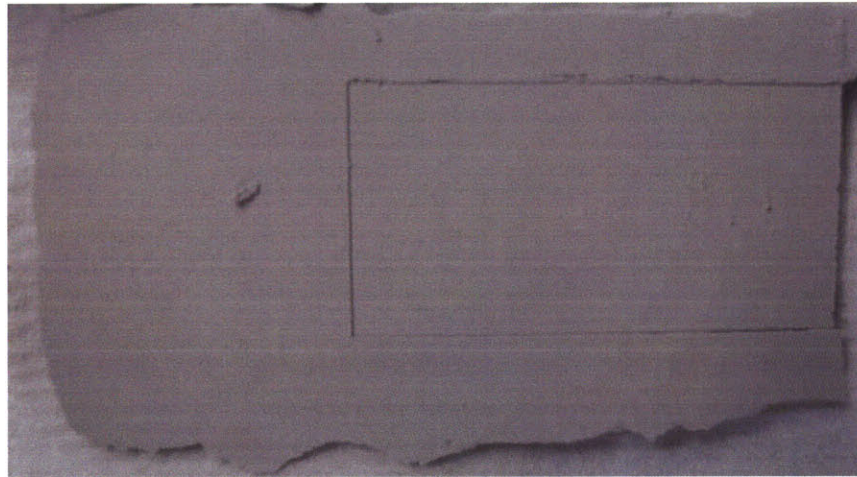


Figure A11: Photographs of a sintered powder shell created with Alumina/SiC bimodal mixture composed of 30 μm alumina and 2.5 SiC powder.

SiC Bimodal Mixture

The final powder mixture tested was a SiC bimodal mixture composed of 45 μm and 2.5 μm SiC powders. Photographs of the shell are shown in Figure 48. The shell created with this bimodal mixture was the most rigid and durable shell created. The shell remained intact after sintering with no shrinkage or cracking what-so-ever. Additionally, the shell created an excellent imprint of the wafer, while maintaining a superior amount of rigidity. The second photograph of Figure A12 shows a slight void in the shell in the bottom left corner of the imprint. This void is troublesome, but could hopefully be avoided with an improved compaction. Overall, the SiC bimodal mixture is the best candidate for preserving a wafer during recrystallization due to its great shape determination and excellent rigidity.

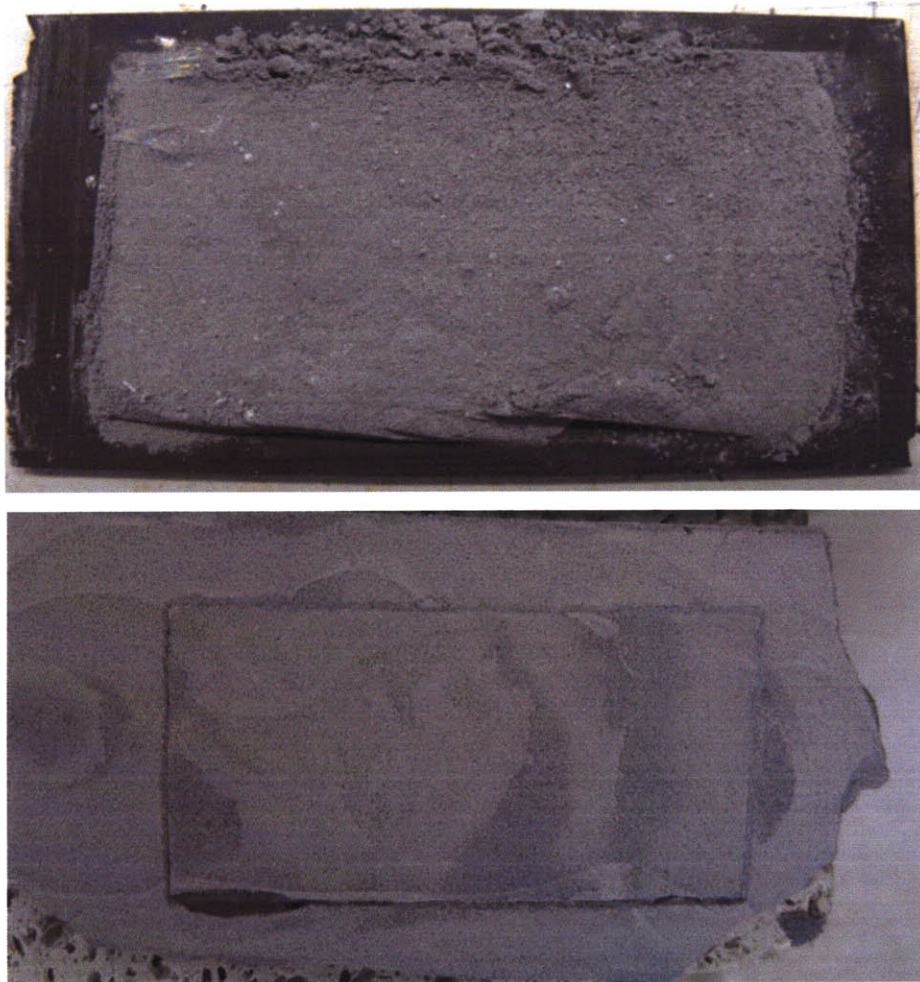


Figure A12: Photographs of a sintered powder shell created with SiC bimodal mixture composed of 44 μm and 2.5 SiC powder.

Powder Comparison

After all powders were tried and their properties recorded, it was then necessary to compare and contrast each powder, deciding which could potentially preserve the geometry of a wafer during recrystallization. Table A1 is a qualitative comparison of all powders tested based on how well they sintered into a rigid shell, and how well they created an intact shell what would encapsulate the wafer. Each powder was given a score of 1 to 5 based on how rigid it became after sintered; 1 corresponding to no sintering and no rigidity, and 5 corresponding to a very rigid structure. Additionally, each powder was given a score of 1 to 5 based on how well it developed a shell that did not crack and a shell that made an imprint of the wafer: 1 corresponding to a cracked shell with no shape determination and 5 corresponding to an intact shell and a perfect imprint of the wafer.

Each powder was compared using this scoring system and only two powders seemed to have sufficient scores to be examined on how well they would actually function in the recrystallization furnace. The two powders chosen to be examined further were the Alumina/SiC bimodal mixture and the SiC bimodal mixture. Both powder mixtures sintered into a rigid shell and created a sufficient mold to potentially preserve the geometry of a wafer during recrystallization.

Powder	Rigidity	Shape Determination	Candidate for Melting Test
<i>Single Constituent:</i>	-----	-----	-----
Silica: 20 μm	1	1	No
Silica: 40 μm	1	2	No
SiC: 15 μm	2	2.5	No
SiC: 44 μm	2.5	3	No
Alumabeads: 10 μm	1.5	4	No
Alumabeads: 30 μm	2	4	No
<i>Bimodal Mixtures:</i>	-----	-----	-----
Silica: 40 μm + Fines	1.5	1	No
Silica: 45 μm + SiC: 2.5 μm	2	2	No
Silica: Fines + SiC: 44 μm	2	1	No
Alumina: 30 μm + SiC: 2.5 μm	3.5	5	Yes
SiC: 44 μm + 2.5 μm	5	4	Yes

Table A1: Table giving a qualitative comparison of all powders tested based on how well they sintered into a rigid shell, and how well they created an intact shell what would encapsulate the wafer. Each powder was given a score of 1 to 5 based on how well it developed a shell that did not crack and a shell that made an imprint of the wafer: 1 corresponding to a cracked shell with no shape determination and 5 corresponding to an intact shell and a perfect imprint of the wafer. This data determined which powders would be tested in the recrystallization process.

Melting Tests

The two selected powder mixtures were then tested in actual recrystallization. The process of creating the shell was done identically to the procedure above, and the final package was then run through the recrystallization furnace. Upon exiting the furnace, each shell was

examined on how well it maintained its structure at the elevated temperature, and how well it encased the molten wafer.

A photograph of a wafer recrystallized with the SiC/alumina bimodal mixture is shown in Figure A13. The powder bed cracked and deformed immensely during recrystallization, resulting in a very non-uniform wafer. The wafer had a scalloped texture and seemed to flow within the cracks that developed in the shell. Overall, the powder mixture was unable to survive the recrystallization furnace. An important result of this trial is that a completely rigid shell is needed to preserve wafer geometry. When the wafer becomes molten, it can translate and infiltrate a non-rigid powder bed, resulting in unsuccessful geometry control of the recrystallized wafer.



Figure A13: Photograph of the underside of a wafer that was recrystallized with a SiC/alumina bimodal powder shell. The resultant wafer has a scalloped texture. The test implies that a completely rigid powder shell is needed to contain a wafer during recrystallization.

The SiC bimodal powder was also tested in recrystallization with photographs of the results shown in Figure A14. The SiC bimodal powder withstood the recrystallization furnace extremely well without cracking. The result was a successfully recrystallized wafer as shown in the second photograph of Figure A14. The shell did an excellent job of maintaining the general shape of the wafer, including excellent control of the horizontal geometry.

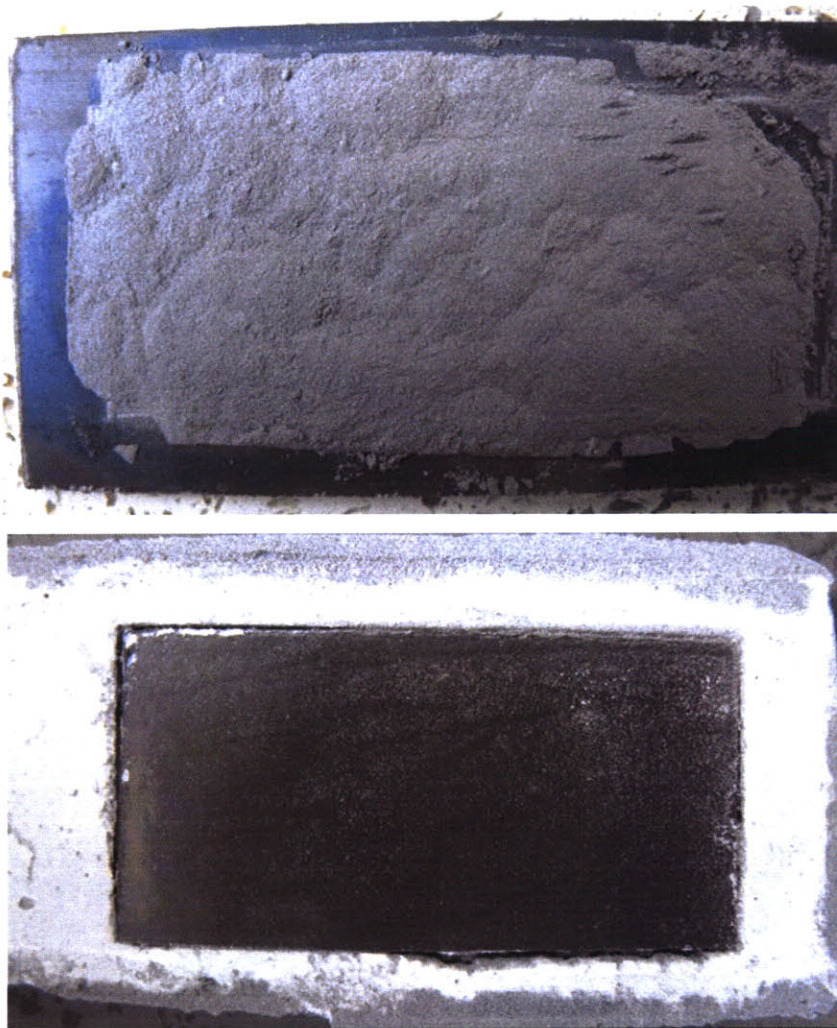


Figure A14: Photographs of a SiC/alumina bimodal powder shell after a recrystallization trial. The shell remained intact and encased the wafer during the process. The wafer remained intact and was subsequently removed from the shell with a hydrofluoric acid solution. This trial demonstrated a successful recrystallization with a powder shell.

The SiC bimodal powder shell composed of a 1:3 ratio of 44 and 2.5 μm powders is the optimal powder to be used in the recrystallization process. Importantly, the powder was composed of high-purity SiC powder, which will not present impurities to a wafer during recrystallization. The shell sintered into a rigid structure, creating an enclosure capable of retaining the molten wafer, and durable enough to withstand the harsh temperatures of the recrystallization furnace. Overall, the shell proved successful in a recrystallization test, and will be improved further for implementation in the recrystallization production process.